

Review

The State of the Art of Photovoltaic Module Cooling Techniques and Performance Assessment Methods

Insan Okta Harmailil ¹, Sakhr M. Sultan ¹, Chih Ping Tso ^{2,*}, Ahmad Fudholi ¹, Masita Mohammad ¹  and Adnan Ibrahim ¹ 

¹ Solar Energy Research Institute, Universiti Kebangsaan Malaysia, Bangi 43600, Malaysia; p134180@siswa.ukm.edu.my (I.O.H.); sakhr@ukm.edu.my (S.M.S.); a.fudholi@ukm.edu.my (A.F.); masita@ukm.edu.my (M.M.); iadnan@ukm.edu.my (A.I.)

² Faculty of Engineering and Technology, Multimedia University, Jalan Ayer Keroh Lama, Melaka 75450, Malaysia

* Correspondence: cptso@mmu.edu.my

Abstract: Due to its widespread availability and inexpensive cost of energy conversion, solar power has become a popular option among renewable energy sources. Among the most complete methods of utilizing copious solar energy is the use of photovoltaic (PV) systems. However, one major obstacle to obtaining the optimal performance of PV technology is the need to maintain ideal operating temperature. Maintaining constant surface temperatures is critical to PV systems' efficacy. This review looks at the latest developments in PV cooling technologies, including passive, active, and combined cooling methods, and methods for their assessment. As advances in research and innovation progress within this domain, it will be crucial to tackle hurdles like affordability, maintenance demands, and performance in extreme conditions, to enhance the efficiency and widespread use of PV cooling methods. In essence, PV cooling stands as a vital element in the ongoing shift towards sustainable and renewable energy sources.



Citation: Harmailil, I.O.; Sultan, S.M.; Tso, C.P.; Fudholi, A.; Mohammad, M.; Ibrahim, A. The State of the Art of Photovoltaic Module Cooling Techniques and Performance Assessment Methods. *Symmetry* **2024**, *16*, 412. <https://doi.org/10.3390/sym16040412>

Academic Editor: Vasilis K. Oikonomou

Received: 13 February 2024

Revised: 5 March 2024

Accepted: 12 March 2024

Published: 1 April 2024



Copyright: © 2024 by the authors. Licensee MDPI, Basel, Switzerland. This article is an open access article distributed under the terms and conditions of the Creative Commons Attribution (CC BY) license (<https://creativecommons.org/licenses/by/4.0/>).

Keywords: PV cooling; classification of PV cooling; assessment methods; temperature reduction; electrical efficiency

1. Introduction

Environmental considerations constitute a major factor in encouraging the use of renewable energy sources. Environmental degradation has resulted from widespread industrial activity and greatly increased pollution levels. The need to develop cleaner and more sustainable alternatives has intensified with recognition of the negative effects of the combustion of fossil fuels, such as airborne pollutants and greenhouse gas emissions that lead to climate change. Furthermore, it is becoming clear that renewable energy has to be developed for superior future energy sources and economic [1,2].

Investments in renewable energy technology have opened doors for economic expansion, technological development, and employment creation. The growing field of renewable energy has attracted the attention of both public and corporate organisations due to its potential for advancement and competitiveness. Furthermore, the need to lessen reliance on imported fossil fuels has been generated by the geopolitical environment. By diversifying their energy sources, countries have attempted to achieve energy security and independence while lowering their exposure to the supply disruptions, price volatility, and political unrest that come with using fossil fuels [3,4]. The creation of domestic renewable energy sources by specific application of solar energy offers a way to attain energy independence.

Solar energy uses the energy from the sun to create thermal energy, distilled water, and electricity. With a variety of uses, it offers a dependable and sustainable substitute for conventional energy systems that rely on fossil fuels [5]. The main utilization of solar

energy is the production of electricity using photovoltaic (PV) systems. Through the use of the PV effect, solar panels equipped with photovoltaic cells directly transform sunlight into electricity. Households, companies, and perhaps entire communities can be powered by this sustainable and clean energy generation [6]. To take advantage of the copious solar energy available, solar PV systems can be integrated into different types of structures, mounted on rooftops, or placed in solar farms. Although PV systems must be installed directly in open daylight areas, the module performance itself will be reduced due to excessive temperatures caused by solar radiation.

These high temperature effects may cause negative impacts on the electrical characteristics of PV. PV modules show the best performance at cooler temperatures, and degrade as temperatures warm up [7]. PV modules' current increases when temperature increases. On the other hand, the voltage at the PV module's output terminals drops as temperature rises. This voltage drop may have an effect on the PV system's overall functionality and power production [8]. The reduced voltage output causes overall power output decrease as a result of high temperatures. Figure 1 shows the effect of temperature on the solar cell I-V curve [9]. The PV system's effectiveness and performance are impacted negatively by this power loss [10]. Therefore, one of the solutions to this obstacle is to implement PV cooling systems to reduce high temperature effects on PV modules.

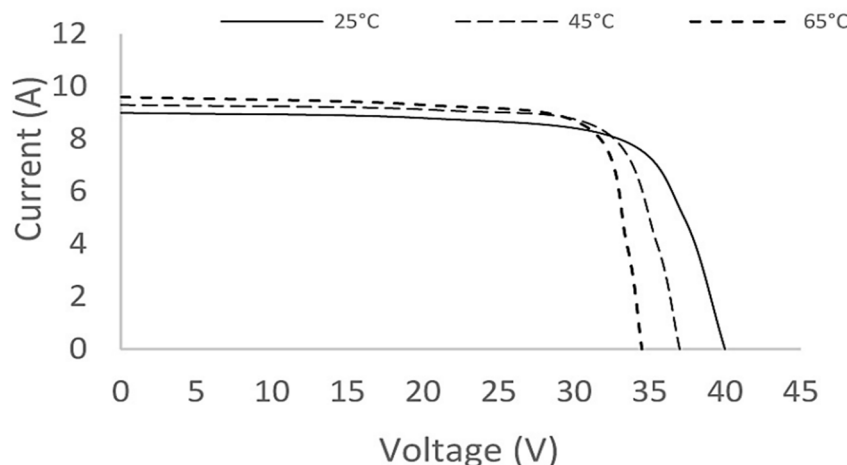


Figure 1. Effect of temperature on solar cell I-V curve [9].

To encourage further advances in PV cooling technology, a comprehensive review of papers detailing current cooling techniques is essential. Because of the possible advantages of increased energy efficiency, cost savings, and environmental preservation, researchers have been actively investigating a range of cooling strategies to improve the efficacy and cost-efficiency of PV modules. Owing to this surge in interest, numerous studies on PV cooling techniques have been carried out. Numerous thorough review studies include in-depth discussions of particular techniques, namely phase change materials (PCM), nanofluid, water, air, thermoelectric cooling, and passive [11–17].

The performance analysis is typically the focus of the standard review of PV cooling. However, there is rarely discussion of the crucial and accepted indicators to assess the effectiveness of photovoltaic cooling techniques, such as the temperature-dependent PV efficiency difference factor (F_{TDED}), temperature-dependent photovoltaic power difference factor (F_{TDPD}), PV power difference factor (F_{ED}), power ratio (R), PV cooler lifespan efficacy factor (F_{LSE}), production cost effectiveness factor (F_{CE}), and modified production cost effectiveness factor (F_{MCE}), which are variables that can impact PV cooling performance. A discussion of these indicators will be given in Section 3.4.

This review article will elucidate several cutting-edge research efforts and developments in PV cooling technology. The comprehensive categorization of PV cooling methods encompasses passive, active, and combined cooling approaches. Additionally, various

performance assessment techniques are presented to evaluate the efficacy of PV cooling methods across different criteria. These two primary subjects will facilitate researchers in identifying and analysing advances in PV cooling technologies. To convey clear and concise information to readers, detailed explanations and examples are provided for each PV cooling classification, along with insights from previous studies. Furthermore, a detailed explanation of the assessment methods for PV coolers will be given.

2. PV Technology

The simple mechanism of PV panels, which convert sunlight into electrical power by using semiconductor materials, makes them an especially useful technology. Edmond Becquerel, a French scientist, made the initial discovery of the photoelectric effect when he observed that some materials generate a specific quantity of energy when exposed to sunshine. Over time, researchers improved and expanded on this discovery, which resulted in the creation of contemporary photovoltaic cells that are readily available today. Sunlight causes a silicon atom's top surface to lose an electron, creating a positive area known as a hole. The free electron travels in the direction of the electron-accepting upper n-type layer. As long as there is sunlight, this process keeps going. As seen in Figure 2, attaching a wire between the top and bottom makes a conduit for electrons to travel, producing electric current for devices [18].

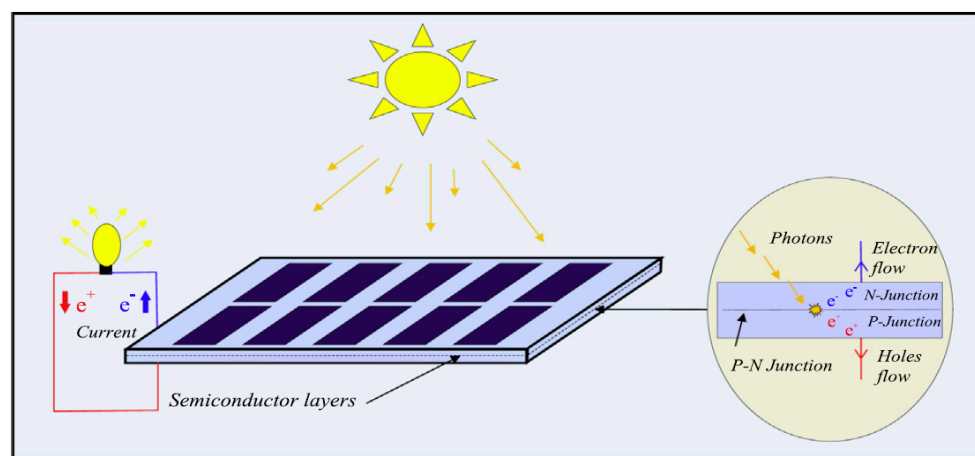


Figure 2. Photoelectric phenomena [18]. Reprinted with permission from Ref. [18]. Copyright 2022 Elsevier.

Recent years have seen tremendous advances in this technology, which has established itself as a well-known renewable energy source with noteworthy advantages such as reduced carbon dioxide emissions, a quick payback period, adaptability to a variety of situations, and durability in adverse environments. Unfortunately, a number of variables that affect it—such as dust accumulation, reflection, angle of inclination variation, orientation, shading effects, radiation exposure, and temperature—cause this technology to display a comparatively lower degree of conversion efficiency [19–25].

3. PV Cooling

Various cooling methods based on cooling processes can be classified as illustrated in Figure 3 [26]. PV cooling can be broadly categorized into two approaches: passive and active. Electric power is not needed for a passive cooling system to carry out its intended cooling of photovoltaic panels. Natural circulation removes heat from the panels. Heat is taken up by cells from the surface and released into the surrounding environment. Active cooling systems rely on external electric power to operate fans or pumps that remove heat from the surface of the panels [27]. Active cooling, which uses active components like fans and pumps, is more effective than passive cooling and has a higher capacity to remove heat from PV panels [16].

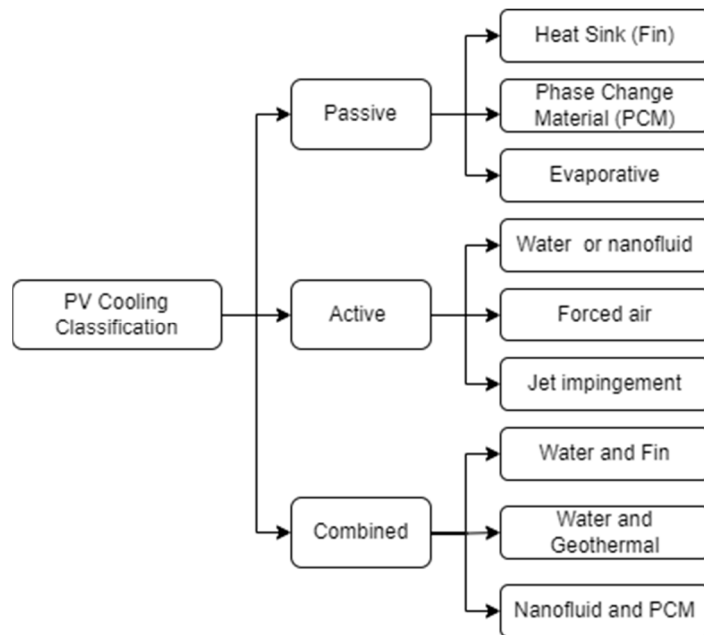


Figure 3. Classification of PV cooling method [26]. Reprinted with permission from Ref. [26]. Copyright 2020 Elsevier.

The third group is merely the combination of particular active and passive cooling methods. Enhancing PV module longevity, performance, and thermal utilisation are the goals. For instance, active techniques with higher thermal recovery capacity and quicker cooling can be mixed with passive techniques with slower cooling. Given that certain cooling techniques release heat after removing it from solar arrays, while other techniques harvest the heat, it is imperative to exercise utmost caution when combining various techniques. Put another way, the ideal situation is to integrate manufacturing processes with techniques that are exclusively utilised for cooling (i.e., without thermal operation) [26].

3.1. Passive Cooling

Passive cooling is defined as a large class of PV cooling techniques that use natural flow with no external power. Pumps are not necessary for passive cooling, which makes use of the natural flow of fluid (water or air) to cool solar panels. Its ability to cool is nevertheless restricted, as the fluid's excess heat needs to be controlled. Because of buoyancy, hot and cold gases exchange heat naturally through convection. For example, the air density decreases when a panel heats up and warms the surrounding air. As a result, hot air rises and a natural convection current is formed. One way to improve natural convection is to increase the heat-transfer area by adding fins [28].

3.1.1. Heat Sink

A metal plate that both absorbs and disperses heat is called a heat sink. Heat sinks can be used in conjunction with forced or natural convection [29]. PV array heat is dispersed using fins on a heat sink [7]. Fins increase the surface area of the heat sink, allowing it to absorb and disperse more heat. In hotter areas, photovoltaic arrays can benefit from this cooling method since the extra surface area helps to keep them cool and effective. Fins are also a crucial part of many systems and gadgets used to enhance air or fluid flow. A number of investigations in fin cooling methods have been performed by scholars.

E. Z. Ahmad et al. (2021) numerically evaluated a truncated multi-level fin heat sink mounted on the bottom of a PV module, taking into account the fin shape [27]. Ahmad et al. examined the thermal performance of truncated multi-level fin heat sink (MLFHS) profiles for PV cooling under natural convection in a numerical simulation. Because of its improved

surface shape, the truncated MLFHS has superior heat transfer performance compared to the rectangular plate-fin heat sink. Their findings indicate that, in comparison to the traditional rectangular design, the truncated multi-level fin heat sink design provided an average temperature that was 6.13% lower. Marinić-Kragić et al. came up with the notion of altering the PV design by creating a slit on a PV panel, whereas the prior study was concentrated on fin geometry. Their straightforward yet efficient adjustment resulted in a 3 °C drop in panel temperature [27,30].

Bayrak and Hakan performed another case study in the Turkish city of Elazig. Ten examples of PV modules, designated A1-A10, were taken into consideration and examined from 9:00 a.m. to 4:00 p.m. in order to study fin numbers and their configurations on a PV panel, as shown in Figure 4. Their research also assumed that the heat transfer coefficient was a linear function of wind speed, therefore they also took the wind effect into account. A design with 26 staggered vertical fins stood out from the rest in terms of efficiency, having maximum energy and exergy efficiencies of 11.55% and 10.91%, respectively. In both horizontal and vertical layouts, instances with 7 cm fin length outperformed those with 12 cm fin length [31].

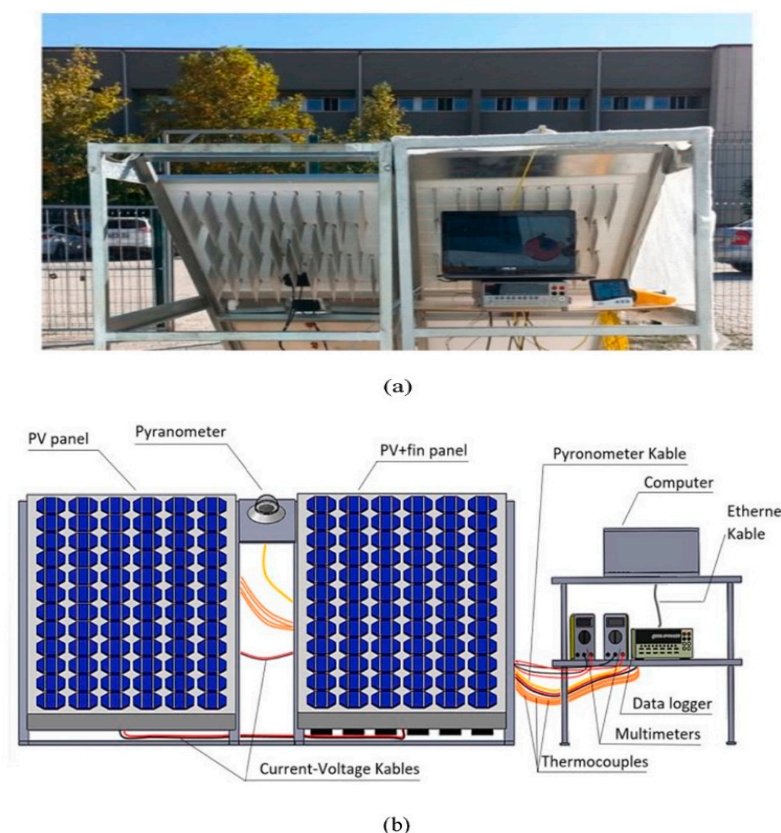


Figure 4. Two views of the experimental setup: (a) real photograph, and (b) schematic view [31]. Reprinted with permission from Ref. [31]. Copyright 2019 Elsevier.

3.1.2. Phase Change Materials (PCMs)

Phase change materials (PCMs), which may absorb significant amounts of latent heat during phase transition processes with little temperature rise, have drawn the interest of certain researchers. Such a PV-PCM module is anticipated to maintain lower temperature of PV cells and achieve improved conversion efficiency by attaching the PCM at the rear of the PV panel. Compared to most standard photovoltaic thermal collectors (PVT), the PV-PCM system requires less maintenance because it uses passive cooling and doesn't require extra electricity or a circulating fluid. Furthermore, a great deal of research has been done to examine the potential applications of PCMs in solar energy and building

energy conservation. They are thought to be an efficient way to use thermal energy from renewable energy sources [32–34].

Sandro et al. have proposed attaching small PCM containers, although nearly all of the articles have considered one solid container covering the entire PV module at the back side. An experimental investigation was conducted in Split, Croatia, where three distinct systems were compared with one another. The second and third were PCM-cooled PV panels with varying configurations, whereas the first was a reference panel. The experimental setup is depicted in Figure 5. It is interesting to note that half of the PCM arrangements outperformed the reference scenario in terms of PV panel performance by 10.7%. On the other hand, the entire PCM setup saw a 2.5% improvement. The innovative PCM container design was a crucial step toward commercializing PCM-cooled PV panels, given the high cost of PCM ingredients. According to their research, their innovative design managed to reduce aluminium by 36% and PCM by 47%. The cooling system's weight was considerably decreased thanks to the high density of organic PCMs. All of these were thought to be essential elements in enabling PCMs to be used to control the temperature of PV panels [35].



Figure 5. Image of the PCM cooling experimental setup [35]. Reprinted with permission from Ref. [35]. Copyright 2021 Elsevier.

Any latent heat thermal storage method must incorporate nanoparticles into basic PCM as a heat transfer augmentation strategy in order to address the issue of most PCMs' low thermal conductivity. Researchers have also looked into other uses for mixing nanoparticles with PCMs. Liu et al. synthesized microcapsules using n-docosane as the PCM core and a $\text{CaCO}_3/\text{Fe}_3\text{O}_4$ shell surface. In comparison to the equivalent microcapsules without Fe_3O_4 , the photothermal conversion efficiency was 47.9% higher in the shell with Fe_3O_4 nanoparticles present. In a different study, the shell of a comparable microcapsule was made of black phosphorus nanosheets. The emulsion's stability enhances the microcapsule system's high latent heat capacity and heat transfer, making it easier to produce tight CaCO_3 -based shells. Photothermal and magnetocaloric conversion were synergistically performed by Fe_3O_4 nanoparticles with magnetic characteristics that were in the $\text{Fe}_3\text{O}_4/\text{CaCO}_3$ composite shell of the microcapsule system [36].

PCM functions similarly to a rechargeable thermic battery. When it comes to absorbing thermal energy, PCMs are comparable to the phase transition from solid to liquid at constant temperatures. Their huge latent heat capacity results in an isothermal phase change. As a result, they can be used to regulate the PV modules' temperature. Calcium chloride hexahydrate ($\text{CaCl}_2 \cdot 6\text{H}_2\text{O}$) was investigated by Rezvanpour et al. as a PCM to control PV module temperature and enhance electrical performance. According to experimental results, the PV-PCM system had the largest temperature drop of 26.3°C , or 38%, when compared to the non-PCM mode. However, the PV-PCM system was able to boost the output power by roughly 1.16 W, or 24.68%. The PV-PCM sandwich model is depicted in Figure 6 [37].



Figure 6. PV-PCM system [37]. Reprinted with permission from Ref. [37]. Copyright 2020 Elsevier.

The application of PCM cooling in bifacial PV modules has been investigated by Abou-Elnour et al. from Monsoura University, Egypt. The goal of the work was to create a bifacial PV-PCMs system made up of several PCMs, a ribbed aluminium plate, and two mono-facial PV cells, as shown in Figure 7. The PV cells' electrical and thermal performance were improved by using ribbed aluminium plates and a variety of PCMs with varying melting temperatures. Three scenarios were investigated for the bifacial PV-PCMs system: a smooth unit using a single PCM (RT-35); a ribbed unit with multiple PCMs (RT-35, RT-27); and lastly, a reference bifacial case without cooling to obtain the best design [38].

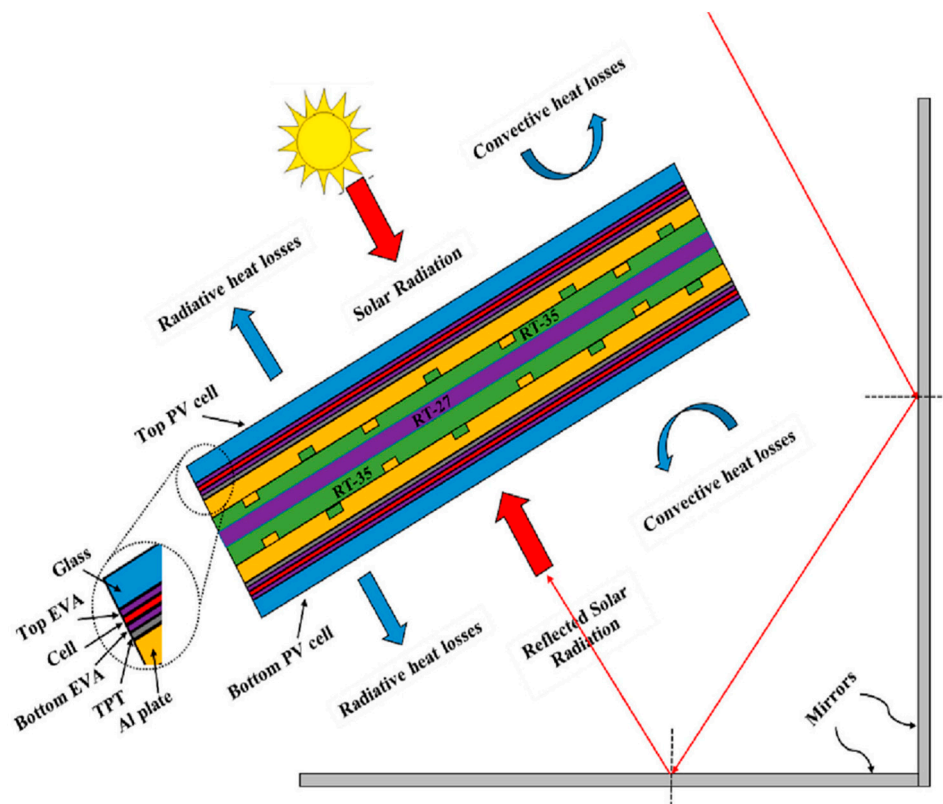


Figure 7. The schematic diagram of bifacial PV-PCMs system [38]. Reprinted with permission from Ref. [38]. Copyright 2023 Elsevier.

The numerical model and data from the literature agreed very well. The system's electrical efficiency and cell temperature were investigated numerically at three distinct solar radiation levels (800, 1000, and 1200 W/m²). The outcomes showed that, in comparison to the smooth case with a single PCM, the top cell electrical efficiency rose by 0.5% in the ribbed case with multiple PCMs. In addition, the temperature of the cell in the suggested system is significantly lower than that of the bifacial cell without cooling—roughly 13 °C. In the ribbed unit with numerous PCMs, the cell electrical efficiency is around 16.68%, whereas in the bifacial case without cooling, it is 15.5% [38]. Another credit to multi-layer PCM performance has been highlighted in both modelling and experimental work. Ranawade and Nalwa discovered that the results of their multilayer PCM experiments indicated that the maximum temperature of the PV module was 7.2 °C and 4 °C lower than that of the single-layer PCM and PV reference, respectively [39].

In another study, Maghrabie et al. examined experimentally the correlation between PCM thickness and PV panel tilt angles. The study looked at the experimental cooling of a PV panel utilizing paraffin wax RT-42 PCM glued to the panel's back surface. For the purpose of outdoor trials, two identical PV panels with a maximum electrical generated power of 40 W were used: a reference PV panel (PVr) and another integrated with PCM (PV-PCM). The PV panels' tilt angles were varied at 15°, 20°, 25°, and 30°, with PCM thicknesses of 1, 2, and 3 cm in the system studied. The results demonstrated that the lower half of the PV panels displayed the lowest temperature dispersion, while the upper section of the panels displayed the highest temperature spread. For PCM thicknesses of 1, 2, and 3 cm, respectively, the temperature at the top side of the panel is higher than the bottom side by 17.1%, 15.7%, and 13.2% at a tilt angle of 15°. Additionally, at a 30° tilt angle, the PV-PCM panel with a 3 cm PCM thickness exhibits a 15.8% increase in electrical power production over the reference PV [40].

3.1.3. Thermosyphon

The idea of thermosyphon cooling, which can function independently of an external power source, is presented. Thermosyphon cooling is based only on the decrease in liquid density following heat absorption, which creates buoyant force that pushes the liquid up in the riser and down in the downcomer. The heat sink's heat is extracted and stored in the water tank by the thermosyphon cooling module, which uses the thermosyphon effect to propel water flow. This innovation improves the system's stability and dependability by producing an effective cooling performance [41].

Moradgholi et al.'s paper described the construction of a unique two-phase closed thermosyphons (TPCTs) system that produces thermal and electrical power concurrently. The thermal system's operating fluids were methanol and Al₂O₃ (methanol nanofluid). Experimental research was performed to determine the impact of filling ratio (at levels of 30, 40, 50, and 60%) and Al₂O₃ nanoparticle concentration in the working fluid (at values of 1.0, 1.5, and 2 wt%) on the module's electrical and thermal performance. The filling ratio and nanoparticle concentration were found to be optimal at 50% and 1.5 weight percent, respectively, based on the results. Under these circumstances, the PV module produced 1.42 W more electrical power output, and had a panel temperature that was 14.52 °C lower, than a normal PV panel of the same kind. Additionally, the system's energy and exertional efficiency were computed. In comparison to a typical PV module, the average electrical energy, average total energy (including thermal efficiency), and total energy efficiency for PVT modules operating with nanofluid at ideal operating conditions, rose by around 1.0%, 27.3%, and 1.1%, respectively [42].

3.1.4. Thermoelectric Generator

Thermoelectric Generators (TEGs) can directly convert waste heat into energy through the Seebeck effect, therefore they may be a useful option in this regard. More significantly, TEG has a lot to offer since it is highly reliable and solid-state, meaning it has no moving parts [43]. As illustrated in Figure 8, thermoelectric generators (TEGs) are electrical gener-

ating devices that directly transform thermal energy into electrical energy by utilising the Seebeck effect and profiting from temperature variations. The two different thermoelectric (TE) materials used in these generators are n- and p-type semiconductors. The semiconductors are coupled thermally in parallel and electrically in series. In theory, a direct electric current will be produced any time there is a temperature differential between the thermocouples' sides. Consequently, it is worthwhile to investigate the possibility of TEGs producing electricity whenever heat transfer from hot to cold sources happens [44–46].

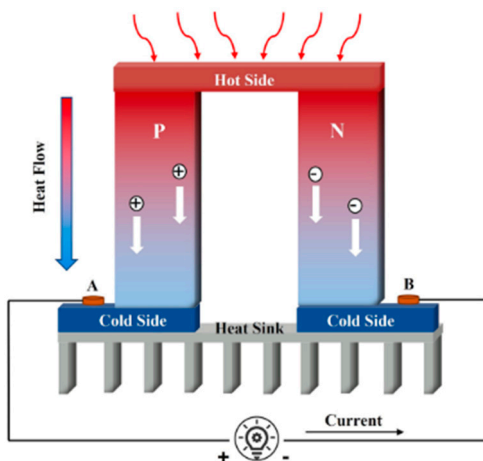


Figure 8. Working principle of TEG [44]. Reprinted with permission from Ref. [44]. Copyright 2024 Elsevier.

Numerical analysis of the linear Fresnel concentrated PV–TEG system with and without heat pipe (HP) allowed investigation and optimization of the structure and performance of concentrated PVT [47]. According to the findings, concentrated PV–TEG with HP had electrical and energy efficiency of 2.91% and 1.56%, respectively. While the thermal efficiency and total efficiency were 10.23% and 2.55% higher, respectively, these efficiencies were lower than those without HP. On the other hand, a thorough theoretical and experimental feasibility examination of concentrated PV–TEG was carried out by Yin et al. The outcomes showed that compared to double-junction GaAs cells, single-junction GaAs cells were more suited for coupling with TEG modules. It should be mentioned that in a concentrated PV–TEG system, the cell temperature cannot be kept at the appropriate operating temperature by a direct connection between the concentrated PV and TEG module [47].

Furthermore, passive cooling methods, such as heat pipes and thermoelectric devices, have also been studied for concentrated PV (CPV) cooling. For the purpose of cooling triple-junction cells, Wang et al. created three-dimensional oscillating heat pipes (Figure 9). The experimental findings demonstrated that a 40 W input power could maintain the CPV cell temperature below 330 K. At comparatively low operating temperatures, CPV cells can be controlled by heat pipe cooling. However, this results in an uneven distribution of temperatures on the CPV cell surface, which lowers the cell's conversion efficiency even more [43]. In this case, thermal management of CPV cells entails both extracting the waste heat from the cell and effectively using it. The system is made up of a Fresnel lens, secondary concentrator, TEG module, vapor chambers (VCs), collector tubes, water tank, and pump. The triple-junction cell module receives homogeneous illumination from the sunlight concentrated by the Fresnel lens and secondary concentrator, as shown in the illustration. A portion of this concentrated sunlight is transformed into electrical energy by the cell module.

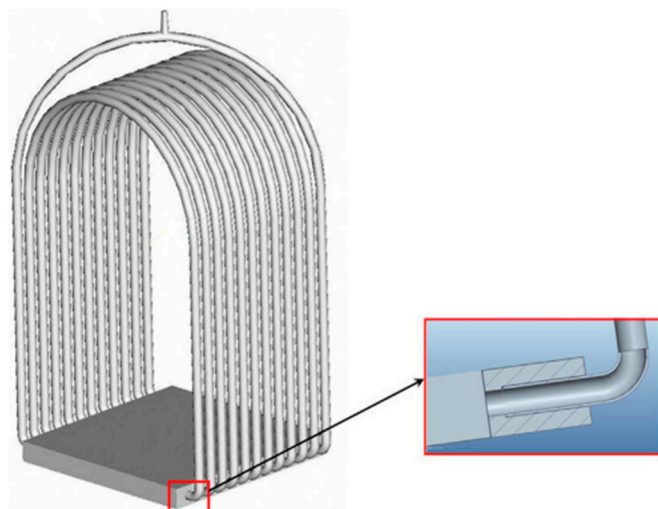


Figure 9. Design of three-dimensional oscillating heat pipe [43]. Reprinted with permission from Ref. [43]. Copyright 2020 Elsevier.

Lastly, Yaya et al. found that in contrast to TEG curves, CPV total electrical efficiency curves exhibit the reverse trend. This is due to the fact that when solar radiation rises, TEG converts more heat into electrical power; as a result, the TEG module's electrical efficiency increases. However, as solar radiation increases and cell temperature rises, the CPV electrical efficiency falls. The overall CPV electrical efficiency follows the same pattern of change since a greater percentage of the CPV electricity generated is included in the total power. The working of this system is detailed in Figure 10 [48]. Table 1 shows some of the recent studies in passive cooling development.

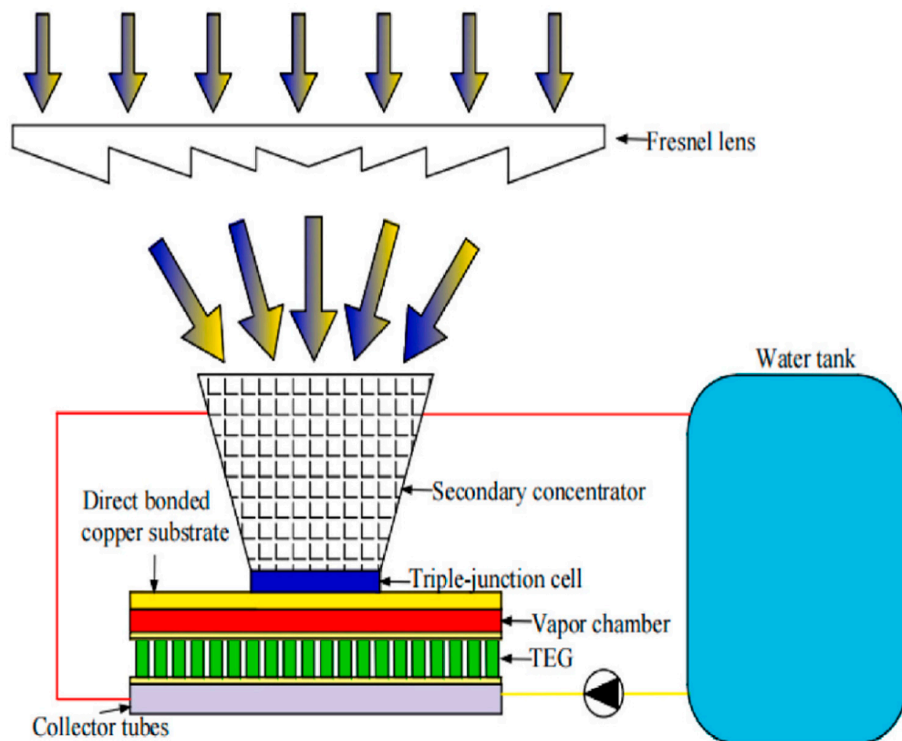


Figure 10. Sectional view of VC and TEG system [48]. Reprinted with permission from Ref. [48]. Copyright 2023 Elsevier.

Table 1. Comparison of Passive Cooling systems.

PV Cooling Classification	Cooling Method Specification	Temperature Reduction	Electric Performance	Innovative Discovery	Reference
Passive Air Cooling	Truncated multi-level fin heat sinks (MLFHS)	MLFHS design gives an average temperature that is around 6.13% lower.	2.87% improvement in the PV module's electrical output power.	Because of its improved surface shape, the truncated MLFHS has superior heat transfer performance to the rectangular plate-fin heat sink. Better flow patterns are shown in the suggested fin design, and the suggested shape creates an abrupt transition within the boundary layer in the fin confined region.	[27]
Passive Air Cooling	Module with fins and a planar reflector	Temperature reduction by 8.4 °C.	Electrical efficiency of 10.68%.	Cooling PV module using passive technique, particularly with lapping fins design, is concluded to be the preferred option over longitudinal fins design due to its simplicity and low cost.	[49]
Passive Air Cooling	Aluminium heatsinks with straight and inclined fin design	Temperature reduction was approximately 9.4 °C and 10 °C, respectively.	Electrical efficiency reached more than 4% for these cooling methods.	In order to improve convective heat exchange and lower pressure losses across heatsink channels, the work suggests a new fin pattern for PV module passive heatsinks. This fin array will also help cool down the PV system by increasing vortex formation.	[50]
Passive PCM Cooling	PCM with RT55 paraffin wax material and 2% Alumina nanoparticles addition to pure PCM	Temperature reduction results are 8.1 °C and 10.6 °C, respectively.	Cooling system's efficiency increased by 5.7% and 13.2%, respectively.	The work bridges the gap regarding the potential application of PCM and nanoparticle compounds in the integrated PV building system's thermal management. Therefore, the purpose, uniqueness, and innovation of the work are to experimentally explore the impacts on temperature regulation and system efficiency increases of the addition of nanomaterial to the PCM in PV integrated systems.	[51]
Passive PCM Cooling	PCM calcium chloride hexahydrate ($\text{CaCl}_2 \& 6\text{H}_2\text{O}$) based system.	Temperature drops by 26.3 °C or 38%.	Boost the electricity output roughly to 1.16 W, or 24.68%.	The phase change material used by the authors is $\text{CaCl}_2 \& 6\text{H}_2\text{O}$ because it is significantly less expensive than other types of PCMs. Further benefits of this material include its large fusion heat capacity, appropriate melting and freezing temperature range for both cold and warm climates, stronger thermal conductivity than paraffin-based PCMs, and availability.	[37]

Table 1. Cont.

PV Cooling Classification	Cooling Method Specification	Temperature Reduction	Electric Performance	Innovative Discovery	Reference
Passive PCM Cooling	Computational model to predict PV-PCM temperature interface.	The average temperature of the period of high incidence (10:00 to 15:00) are 39 °C, 39.5 °C, and 44 °C for Computer Fluid Dynamic (CFD), enhanced conduction model (ECM), and conduction model.	The highest average efficiency is up to 18%.	Develop a computational investigation to simulate the PV-PCM temperature interface as an accurate prediction while reducing the computational time with ECM and CFD.	[52]
Thermosyphon passive cooling	Two-phase closed thermosyphons (TPCTs) with methanol and Al ₂ O ₃ (methanol nanofluid).	Lowering temperature by 14.52 °C.	The PV cell produced an extra 1.42 W electric power.	The work uses nanofluid in TPCTs. Furthermore, effect of filling ratio and nanofluid concentration to achieve optimal performance of cooling is discussed.	[42]
Thermoelectric Generator (TEG)	High CPV with vapor chamber and TEG.	Temperature difference of the PV cell with TEG2 and TEG5 are 22.0 K and 12.2 K, respectively.	Electrical efficiency increased by 0.36% and 2.72% with TEG2 and TEG5, respectively.	TEG module is used to recover the waste heat from the cell, which is transferred by the Vapor Chamber (VC), to improve the utilization of solar energy.	[48]

3.2. Active Cooling

Active cooling is defined as another main class of PV cooling which utilizes mechanical assistance (such as fans, pumps, suction devices, etc.) to enhance the coolant's contact flow and boost heat transfer. Using pumps to create forced water flow, active cooling modifies the speed of the water to control panel temperature [28].

3.2.1. Water and Nanofluid Cooling (Liquid Cooling)

Liquid cooling is one of the major and most common methods of PV cooling. Generally, there are two ways to use liquid cooling in active mode: either the liquid (water and nanofluid) flows through the area behind the PV modules, or a thin film of liquid passes through the facing area of the modules [26]. This technique provides greater and more progressive heat removal than other methods. The development of this method has expanded into various methods to reduce PV temperature by water, such as jet impingement, water spray, water pipe, thin-water film, microchannel, and also in combination with another cooling method.

One of the direct methods in liquid cooling is called spray cooling, which affected the performance of the panels examined by Yesildal, et al. Spraying duration, spray velocity, nozzle air stream rate, nozzle-to-panel distance, and solar irradiation were the parameters analysed (Figure 11). Following that, 32 tests were conducted in accordance with the experimental schedule that was produced using the Response Surface Method. Consequently, 49.8990 s for spraying time, 0.0180 m³/h for spray flow rate, 2 m³/h for nozzle air flow rate, 50 cm for nozzle-to-panel distance, and 700 W/m² for solar irradiation, were found to be the optimal values for maximum electrical efficiency. It was found that the spray flow velocity, spraying period, and solar irradiance were the most important characteristics [53].

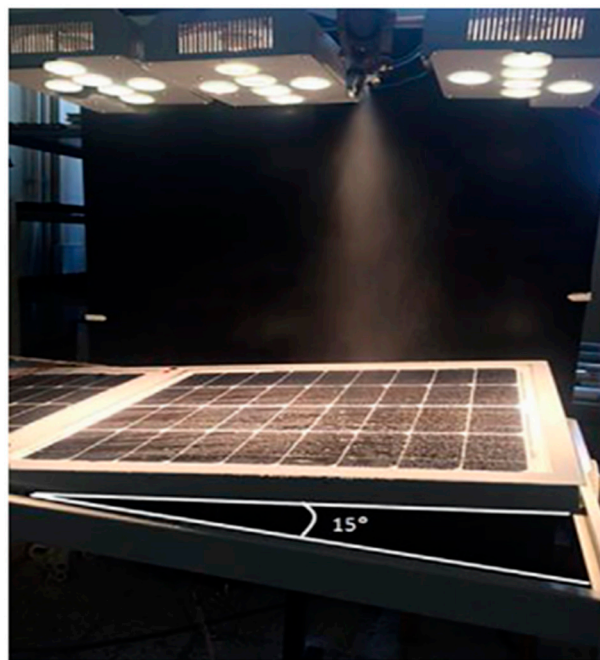


Figure 11. Position of PV cell and water spray cooling in the experiment [53]. Reprinted with permission from Ref. [53]. Copyright 2022 Elsevier.

In contrast to the majority of the literature, Kemal et al.'s experimental investigation used a flowing water layer to cool the PV panel's upper surface (Figure 12). As a result, dusting of the PV panel surface can be avoided. It has been established that the cooled solar panel produces more power than one that is not cooled. By using the specified cooling system, the average power increase was around 9.51%. Consequently, it was stated that the efficiency of the cooled solar panel was roughly 13.69% higher than that of the uncooled one. The average power output of the PV solar panels, cooled and uncooled, was found to be 127.69 W and 116.55 W, respectively. In addition, the panel with water film flowing across it had a lower bottom surface temperature than the panel without cooling. The average bottom surface temperatures of the cooled and uncooled panels were found to be 28.21 °C and 30.09 °C, respectively [54].

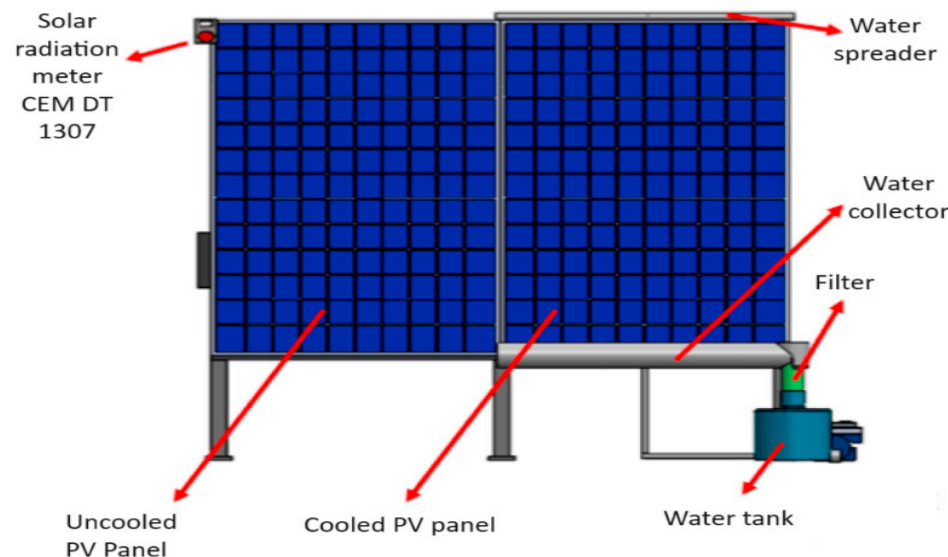


Figure 12. Schematic diagram for uncooled PV cell and cooled PV cell with thin water film (front view) [54]. Reprinted with permission from Ref. [54]. Copyright 2023 Elsevier.

In order to achieve a practically acceptable electrical efficiency in a difficult environment, Shamroukh and others studied a thin-film photovoltaic panel. Copper pipes, which are mounted to the rear of the panel, allow cooling water to flow through them. The heated water from the output then travels through the heat exchanger and its tank to the DC pump. The experimental setup can be seen in Figure 13. Using the suggested cooling system, the PV panel efficiency was experimentally studied. The experimental findings showed that, in the absence of cooling, the daily average efficiency only reached about 6.2%, but with the open-loop system, it increased to 11.3% [55].

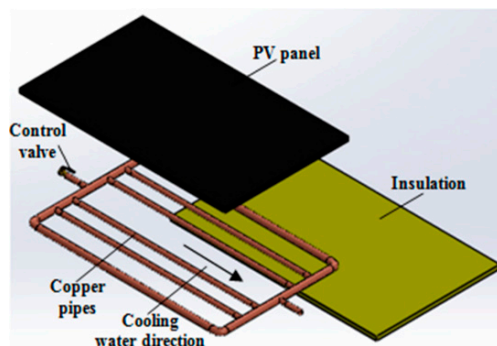


Figure 13. Open-loop water cooling system [55]. Reprinted with permission from Ref. [55]. Copyright 2019 Elsevier.

Irwan et al. conducted an indoor test to investigate the performance of PV panels that used a water-cooling approach. They made use of a solar simulator that mimicked sunshine through the use of a halogen lamp bulb. They found that by using this cooling system, the output power rose by 9–22% and the operating temperature dropped by a range of values from roughly 5 to 23 °C. They also came to the conclusion that the panel efficiency had increased as a result of their suggested cooling solution. Its lifespan increased and the payback period of the investment system shortened [56]. Rahimi et al. conducted an experiment using water as a cooling fluid in single and multi-header microchannels for photovoltaic cooling. Their experimental results showed that utilizing a multi-header microchannel reduced the PV panel's surface temperature by about 6.8%. On the other hand, a single-header microchannel reduced the heat by 19% [57]. Furthermore, by employing a cooling-water system, Peng et al. experimentally increased the output energy efficiency of a solar PV panel. Their data showed that, in the specified cooling environment, the solar PV efficiency rose by 47% [58].

The system employed by Ebaid et al. presented another water-based cooling method for PV panels. They used two combinations in an experimental investigation to cool a photovoltaic panel. The first was an Al_2O_3 –water nanofluid with a mixture of cetyltrimethylammonium bromide and TiO_2 –water nanofluid with a mixture of polyethylene glycol. They proved that the use of nanoparticles, as opposed to pure water, had the effect of lowering the average surface temperature of PV panels. Moreover, the PV panel surface temperature dropped as mixture concentrations and flow rates increased. Additionally, when compared to those using the TiO_2 nanofluid mixture and pure water, the Al_2O_3 nanofluid mixture produced the best increase in power and efficiency as well as the best reduction in the surface temperature of the PV panels [59]. In addition, a PVT system's performance in summertime was assessed by Nardi et al. A polycrystalline photovoltaic panel and a basic solar concentrator made up their suggested setup. The total efficiency using standalone PV panels with cooling or hot-water production improved by more than 28% over bare PVT [60].

An innovative method for enhancing the performance of solar systems is jet impingement water cooling. This method effectively dissipates heat, assisting in temperature control and possibly yielding efficiency gains, by directing high-velocity water streams

directly to the photovoltaic components. Using the jet impingement water cooling technique, Bahaidarah and his lab team conducted an experimental evaluation of solar panel performance, as shown in Figure 14. The findings indicated that in June and December, respectively, the uncooled system's temperature was 69 °C and 47.6 °C. The average cell temperature was lowered to 31.6 °C in June and 31.1 °C in July by using jet cooling. In June, jet cooling increased energy output and conversion efficiency by 51.6% and 66.6%, respectively. In a similar vein, December performance improved by 49.6% in power generation and 82.6% in conversion efficiency, according to the data [61].

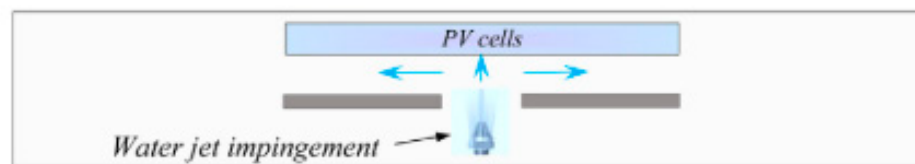


Figure 14. Schematic of the jet impingement cooling system [61]. Reprinted with permission from Ref. [61]. Copyright 2016 Elsevier.

Recent work in novel cooling systems for PV modules using various fluid types has taken pulsating flow, featuring various jet impingement methods, into consideration. The cooling mediums are hybrid nanofluid and alumina–water nanofluid with spherical and cylindrical nanoparticles. When various systems are compared, the pulsating nano-jet cooling system with cylindrical-shaped nanoparticles in an alumina–water nanofluid is found to be the most efficient cooling system. In contrast to an uncooled PV system, a temperature reduction of 37.30 °C was observed at the largest amplitude and highest density of nanoparticles in the pure fluid [62].

Techniques such as cooling channels and water pipes are useful cooling methods for solar power plants. Through efficient heat dissipation from the PV panels, these techniques help to properly regulate temperature and may even enhance performance. A serpentine half tube's performance for PV enhancement was investigated by S. Kianifard et al. (see Figure 15). According to the findings, the suggested model's thermal and electrical efficiencies rose by roughly 10% and 6%, respectively, when compared to the conventional models. These increases corresponded to percentage gains of 3.6% to 5.5%. Cooling tubes can increase the efficiency of power production by more than 13% and decrease the temperature of PV panels by 10–25 °C. The materials and different designs of tubes (full, half, and finned) which can be arranged in serpentine, linear, and circular configurations determine how effective the product is. Multiple cooling approaches, such as fluid-based solutions (air, water, nanofluids) and phase-change material inclusion, can be used in conjunction with this strategy. The majority of these techniques, it should be noted, are classified as active cooling technologies [28,63].

This study looks at the PV cooling system's structural design and parameter optimization. A thermal-electric linked model of the PV cooling system has been drawn up for this purpose. The impacts of many parameters, including the kind of tube, tube diameter, tube spacing, water inlet temperature, and flow velocity, are examined using the mathematical model. The improved PV cooling system may successfully lower the surface temperature, as demonstrated by the test results, which are approximately 47 °C lower than those of the non-cooled system. The mass flow has an exponential relationship with both the conversion efficiency and the exergy efficiency. The greatest values of 11.9% and 12.4% were reached by the conversion and exergy efficiency, respectively, at a mass flow rate of 0.04 kg/s. The greatest values of 11.6% and 11.7%, respectively, were reached by the conversion and exergy efficiency when the water inlet temperature was 10 °C [64]. Meanwhile, Pang et al. conducted an experimental comparison between a traditional glass substrate-based PV system and an aluminium substrate-based water-cooled PVT system. According to their findings, the aluminium-based system outperformed the glass-based one in terms

of electrical efficiency by a factor of twenty. Additionally, the technology they suggested was compact and adaptable in design [65].

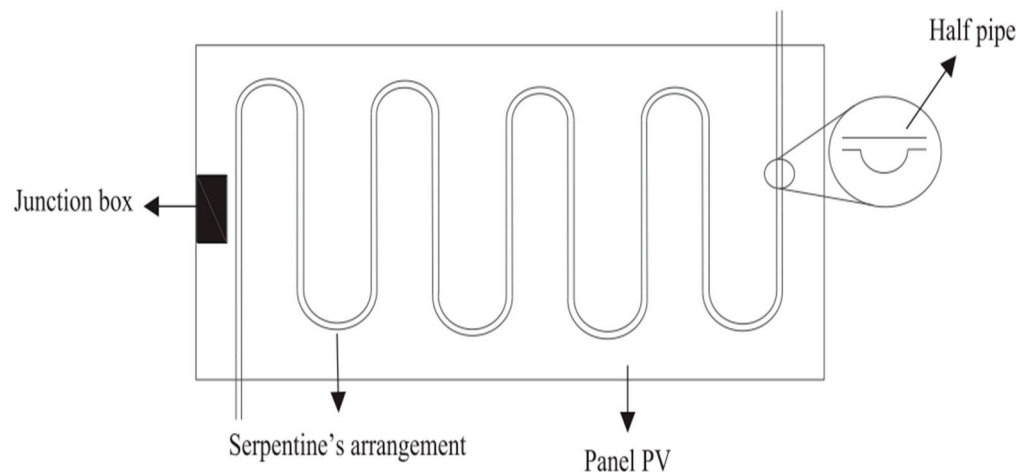


Figure 15. Overview of the connection of serpentine half pipe to PV [63]. Reprinted with permission from Ref. [63]. Copyright 2020 Elsevier.

The application of microchannel cooling has been demonstrated by Alihosseini et al. The work utilized a hybrid arrangement for cooling a high-concentration solar cell by inventive design that came about as a result of an extensive investigation into the integration of an oblique microchannel and a micro-pin fin. With an average water flow rate of roughly 30 and 52 mL/min in the spring and summer, respectively, the solar cell achieved an electrical efficiency of 40.16% while maintaining a cell surface temperature of 301 K when operating under the ideal pattern. In the autumn, the high-concentration photovoltaic cell's total domain output power reached 18.443 W, of which 1.47 W came from pumping power. During the summer's hottest hours, from 11:00 to 17:00, a straight microchannel was unable to maintain a steady cell temperature. However, the hybrid structure, with an average flow rate of 90 mL/min, was successful in maintaining cooling. The greater performance of the hybrid microchannel resulted from flow mixing and a larger wetted surface, which periodically disrupted boundary layers and improved heat transmission [66].

Then, on the hottest day of each season in Shiraz, the effectiveness of a photovoltaic cell with a concentration ratio of 1000 was assessed under real-world boundary circumstances.

3.2.2. Air Cooling

Air cooling is one of the simplest and most direct methods for cooling photovoltaic cells because it is readily available, easy to use, and the price is reasonable. Although it is more expensive than passive cooling methods due to its power consumption, it typically provides superior performance. PV panel efficiency can be increased with forced air flow active cooling. The speed of the fans being used, whether the fan is positioned in front or behind the PV panel, and the surrounding environmental factors, affect how effective forced (active) air flows are at cooling PV [67].

In order to look at how forced air-cooled heat sinks affect PV cell temperatures, Arifin et al. conducted both numerical and experimental analyses. Upon simulating the heat sink model with an air flow velocity of 1.5 m/s, temperature of 35 °C, and heat flux of 1000 W/m², the PV panels' average temperature dropped from 85.3 °C to 72 °C. The PV module's open-circuit voltage and maximum power point increased by 10% and 18.67%, respectively, as a result of the decrease in surface temperature [68]. Rahman et al. examines how well PV modules perform when forced air conditioning and aluminium heat sinks are used. Under the solar cell, a cooling circuit arrangement is constructed to improve the distribution of cold air to the PV panels. It consists of five T-shaped pipes connected to a 6-inch pipe plenum. The study was carried out in real time and on-site

at a public hospital that uses a lot of energy because it operates every day of the year. The PV panels in this study had an average electrical efficiency of 17%, which is quite near to the 19.38% PV module efficiency under standard test conditions (STC). Under nominal operating cell temperature (NOCT) circumstances, the projected solar energy output is 12.35% lower than the actual energy yield observed for the installed PV panel. The study's findings demonstrate that even when utilizing the same solar panel, solar energy generation may be optimized by taking into account design, material usage, and appropriate cooling techniques [69].

Hussien et al. performed research that used forced convection to cool PV panels. Computational fluid dynamics (CFD) was used to analyse the panel temperature distribution and cooling airflow characteristics. The study looked at two distinct cooling techniques: PV panels with forced air cooling that used a blower and a lower duct to deliver air, and PV panels with forced air cooling that used small fans symmetrically mounted on the back side of the PV panels. Eight tiny fans, covering roughly 4.5% of the PV panel's surface area, were fixed to the back of the PV module in this setup. Figure 16 displays a picture of this cooling system along with the locations and separations between the fans. The study found that when PV systems are fitted with distributed cooling fans, they function significantly better than when they use concentrated cooling blowers. The PV module is able to reduce its temperature by approximately 9.9 °C and 5.4 °C, respectively, as a result of the integrated fans and cooling blower. The PV array with distributed fans and blower achieves a maximum total gain in energy savings of 7% and 3.9%, respectively [70].



Figure 16. PV array with fans [70].

Syafiqah and her research group focused on a direct-current (DC) fan-cooled photovoltaic (PV) panel. The PV panel's operational temperature was lowered by installing a DC fan cooling device at its rear. It was discovered that when the DC fan speed increases, the temperature of the PV panel decreases. However, as the DC fan's speed increases, so does its power consumption. While the maximum speed of the DC fan can optimise the power produced by the photovoltaic panel, it also results in the lowest output power savings because the DC fan demands the most input power. Consequently, 3.07 m/s was chosen as the ideal DC fan speed for the cooling system [71]. In the northwest of Iran, Dehghan et al. evaluated the techno-economic aspects of PV air conditioning in two scenarios. The use of three and six low-energy fans differentiates the two scenarios. According to the energy balance calculations, using three fans would result in a higher electrical output. For Scenarios 1 and 2, net specific energy improvements of 4.4% and 4.1%, respectively, were reported. The techno-economic research showed that only at high feed-in tariff rates can the suggested thermal management be easily justified [72].

Lastly, Almuwailhi and Zeitoun used three distinct methodologies to examine the impact of cooling on the performance of poly-crystalline PV panels: (i) natural convection, (ii) forced convection, and (iii) evaporative cooling with forced and natural convection. The results of the experiments indicated that forced convection, with an air speed of 3 m/s, increased the daily energy generation and efficiency of the panels by 4.4% and 4.0%, respectively, while natural convection cooling, with a 120 mm air gap, increased

these values by 1.7% and 1.2%, respectively. The higher convective heat transfer coefficient supported by the air flow velocity was the reason for the greater improvement with forced convection [73]. Table 2 shows some studies of active PV cooling.

3.3. Combined Cooling

Combined cooling is the combination of active and passive cooling to enhance performance, lifespan, and thermal utilisation of PV systems. For instance, active techniques with higher thermal recovery capacity and quicker cooling can be mixed with passive techniques with slower cooling. Given that certain cooling techniques release heat after removing it from solar arrays, while other techniques harvest it, it is imperative to exercise utmost caution when combining various techniques. Stated differently, the optimal scenario involves merging techniques utilised exclusively for cooling, that is, without any thermal operation, with the techniques employed for producing photovoltaic panels [26].

Table 2. Comparison of studies of active cooling.

PV Cooling Classification	Cooling Method Specification	Temperature Reduction	Electric Performance	Innovative Discovery	Reference
Active water cooling	PV cooling with high frequency ultrasound	Increase in cooling efficiency in the range of 2.75–57.25%.	The percentage of maximum power increase in the range of 3.4 to 51.2% related to cold vapor flow rate or ultrasound power.	Applying ultrasonic energy and nanofluid simultaneously is being researched as a potential active cooling technique for PV cells. The use of high frequency ultrasonography to atomize CuO nanofluid is the primary innovative aspect of this work. Thus, the cold vapor, an atomized fluid employed as a cooling working fluid, is produced using high frequency ultrasonic waves.	[74]
Active water cooling	Jet impingement water cooling	Maximum temperature was reduced from 69.7 °C to 36.6 °C and 47.6 °C to 31.1 °C by applying cooling for June and December, respectively.	Power output and conversion efficiency were improved by 51.6% and 66.6% by employing jet cooling for the data of June and December, respectively.	The benefit of utilizing impingement cooling can lead to a low average cell temperature. PV strings' cell temperature, power production, and conversion efficiency may all be examined using the heat transfer analysis for a single nozzle that is performed using the jet impingement geometric model.	[61]
Active water cooling	Water pipe cooling	It reduces the surface temperature, which is about 47.0 °C lower than that of the non-cooled system.	The conversion and exergy efficiencies achieved maximum values of 11.9% and 12.4%, respectively.	The goal of the work is to thoroughly optimize and investigate PV cooling systems. The impacts of many parameters, including the type of tube, tube diameter, tube spacing, water inlet temperature, and flow velocity, are examined using the mathematical model. The findings demonstrate that as tube diameter and flow velocity rise, and as tube interval and water inlet temperature fall, the average surface temperature of the PV cell can be lowered.	[64]

Table 2. Cont.

PV Cooling Classification	Cooling Method Specification	Temperature Reduction	Electric Performance	Innovative Discovery	Reference
Pulsed-spray water cooling		The temperature of PV surface reduces from 57.1 °C to 24.8 °C and 26.5 °C by using the steady-spray cooling system and pulsed-flow cooling system, respectively.	The maximum electrical power output of the PV panel increases about 27.7%, and 25.9% by using the steady-flow water spray cooling system, and the pulsed-spray cooling system, respectively.	In the majority of the examples in the earlier research, the PV panels' temperature was cooled and managed using a cooling system with a steady-flow design. Nevertheless, these systems use a lot of water, which might be a big issue for large-scale PV generating plants. In order to cool the PV panel and use less water in the cooling process, a pulsed-spray water cooling system is devised and tested. The pulsed-spray cooling system reduces water consumption to one-ninth in comparison with the steady-flow cooling system.	[75]
Active air cooling	Forced air cooling with fan and blower	Temperature reduction of the PV cell by about 9.9 °C and 5.4 °C, respectively.	There is an increase of 1.34% in PV panel efficiency.	In order to maintain the cells' temperature as low as possible and boost PV module efficiency, the work attempts to investigate forced air cooling with a small fan and blower.	[70]

Verma et al. employed aluminium fins to cool PV panels and examined a number of methods. The main objective of the study was to cool the solar panel in order to reduce the system's working surface temperature, increase thermal efficiency, and find new uses for the passive energy generated by the heat that the airflow absorbs, as highlighted in Figure 17. The cooling system's aluminium fins were added using three different methods. These methods included the fin arrangement and forced or natural air-cooling flow. To accomplish the forced flow method, air was sent over the fins at different velocities using a variable speed fan. Because of its inexpensive cost, widespread availability, and excellent thermal conductivity, which enhances heat extraction and speeds up the process of removing heat from the PV panel, aluminium fins were chosen. With aluminium fins, the performance and PV efficiency improved in all of these experiments. This improvement lengthened the life and raised the output power. PV modules featuring forced air flow and longitudinal fins proved to be the best solution. One improvement was the use of L-shaped aluminium fins with holes that were affixed to the rear of the PV panel using thermal conductive paste. Analysis revealed that the greatest cooling for the PV panel came from randomly positioned fins with holes on the back side, which allowed air to enter the structure at a natural airflow velocity of 1 m/s. The electrical and thermal performance of PV panels with various types of aluminium fins were compiled. Depending on the fin type, the increase in electrical performance varied from 2% to 18.6% as the PV temperature dropped from 12.5 °C to 7.4 °C [17].

Babu and Ponnambalam thought the impact of wind speed on standalone photovoltaic systems had received more attention than that of hybrid systems. The cooling heat sink capacity significantly improves both systems' performance. The heat sink's attachment beneath the TEG systems is worthy of remark. Through mathematical modelling, the PV-TEG system's performance was investigated. They concluded that a hybrid PV-TEG system might result in a 6% increase in overall efficiency as well as a 5% increase in energy production. Additionally, they reported that a rise in ambient temperature increases the

power consumption of the hybrid PV–TEG system; nevertheless, this has been shown to have a negative impact on the stand-alone PV system [76].

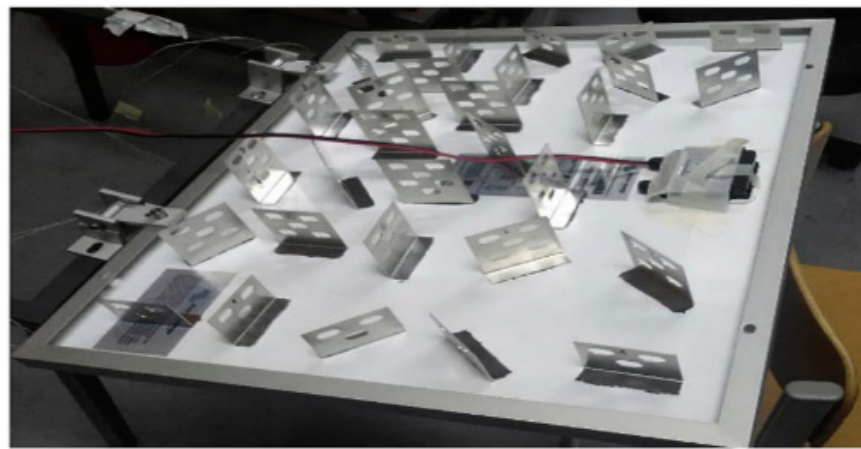


Figure 17. Use of aluminium fins on the back side of PV module [17]. Reprinted with permission from Ref. [17]. Copyright 2018 Elsevier.

Hassan et al. contrasted a PCM and single PCM cooling system with a combined cooling system made up of graphene–water nanofluid and PCM (RT-35HC). The empirical findings showed that the temperature of the PV module decreased by roughly 23.9 °C in the PV/T-PCM system with nanofluid, 16.1 °C in the PV Thermal-PCM system with water, and 11.9 °C in the PV-PCM system. Additionally, compared to PV modules without cooling technology, the electrical efficiency of the cooled modules rose by roughly 23.9% in PV Thermal-PCM systems with nanofluid, 22.7% in PV Thermal-PCM systems with water, and 9.1% in PV-PCM systems. The research verified that the hybrid PV Thermal-PCM system with nanofluid has around 12% higher thermal efficiency than the PV Thermal-PCM system [77].

Yang et al. investigated a cooling system that could transfer heat using shallow geothermal energy. The PV module without a cooling system, the PV module with a cooling system but no shallow geothermal energy, and the PV module with both a cooling system and shallow geothermal energy were tested in three different phases of the experiment. Water is sprayed on the panel's bottom side as part of the cooling mechanism, and the water is then cycled back to a U-shaped borehole exchange tank (UBHE). The setup's design and temperature distribution are displayed in Figure 18. The cooling temperature of the entire system was between 28 and 29 °C, whereas the system without the U-shaped borehole exchanger witnessed a rise to 40 °C. The efficiency of the PV panel with UBHE remained nearly constant at 9.52%, 9.51%, and 9.50% under theoretical analysis with solar intensities of 800–1000 W/m², while the PV panel with only a cooling system had a greater efficiency of 9.17, 13.08, and 14.32%, respectively [78].

In certain areas, air precooling can significantly increase the efficiency of PV thermal management due to high ambient temperatures. Research indicates that this issue can be resolved by air precooling. Elminshawy et al. employed a subsurface heat exchanger for air precooling in their study. Figure 19 shows flexible hoses delivering pre-cooled air to the PV. In their investigation, different flow rates and raised ambient air temperatures of 35, 40, and 45 °C were evaluated to see how they affected the module's efficiency. It was found that the temperature could be effectively regulated by using the heat exchanger. By comparing the panels' output power, it was found that using this cooling technique might increase daily electricity efficiency by as much as 29.11% r [79]. Different studies of combined cooling are given in Table 3.

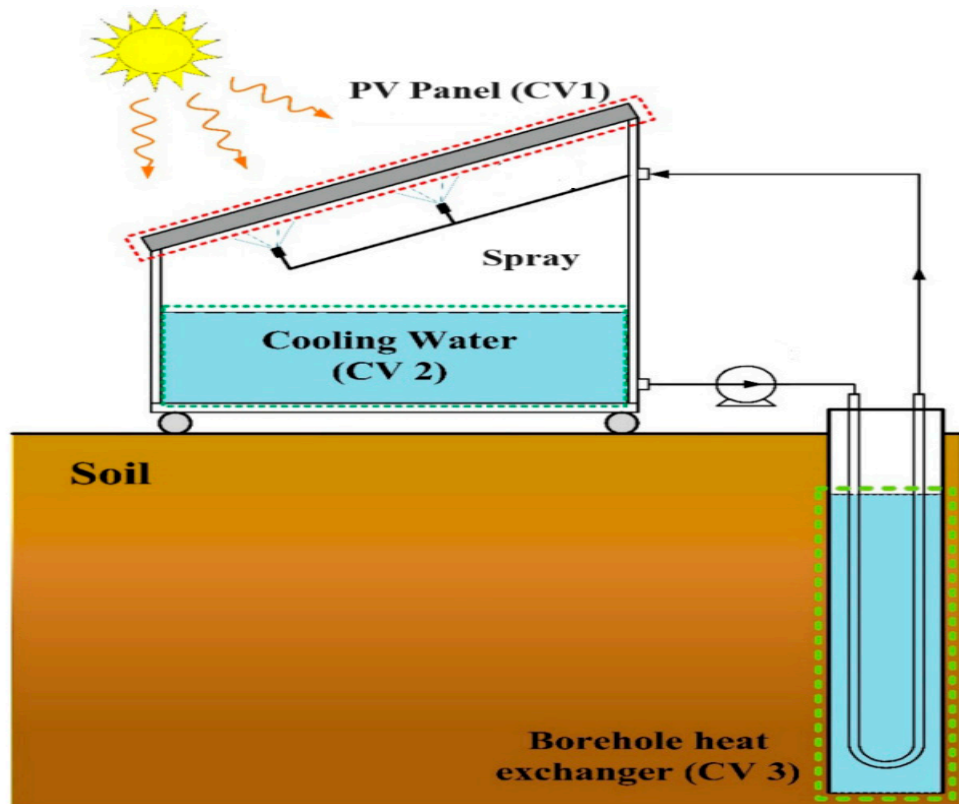


Figure 18. Schematic diagram and temperature distribution of setup [78]. Reprinted with permission from Ref. [78]. Copyright 2019 Elsevier.



Figure 19. Flexible hoses delivering pre-cooled air for the PV [79]. Reprinted with permission from Ref. [79]. Copyright 2019 Elsevier.

Table 3. Recent studies of combined PV cooling.

PV Cooling Classification	Cooling Method Specification	Temperature Reduction	Electric Performance	Innovative Discovery	Reference
Combined Cooling	Air passive cooling and water cooling	It reduces the PV panel's surface temperature to 20 °C.	The result stated an increase in output power of 20.96 W, and 3% in electrical efficiency.	The cooling problem in PV modules may be solved by using a multi-concept cooling technology, which combines two concepts: water passive cooling and air passive cooling.	[80]
	Water-cooling system and PCM combination	The average temperature reduction for four designs, case I, II, III and IV, were 4.35 °C, 3.25 °C, 5.40 °C, and 2.46 °C, respectively.	There was an increase in the average electrical efficiency of PV-PCM by 9.58% compared to the reference PV panel.	The goal of the work was to assess experimentally the cooling capacity of PCM integrated water-based passive cooling technology on PV panel performance enhancement. Based on the direction and duration of the water flow, an experimental comparison of the cooling potential of PV panels with PCM integrated water circulation cooling technology was conducted.	[81]
	Aluminium fins and an ultrasonic water humidifier cooling system	It reduces the temperature of the panel by 14.61 °C on average.	The electrical efficiency of the module improved by 6.8%.	The study increased a PV module's electrical production by combining passive and active cooling techniques. The panel was cooled using an ultrasonic humidifier and an aluminium fin heat sink. A humid atmosphere was created at the back of the PV module using an ultrasonic humidifier.	[82]

3.4. Existing Performance Assessment Methods for PV Cooling Techniques

The main objective of technology aimed at enhancing PV systems is to improve their efficiency. In this section, the evaluation of the effectiveness of different enhancement technologies by assessing their impact on the overall performance of PV systems is considered. Considerations such as the durability, cost-effectiveness, and production efficiency of the enhancer are pivotal in determining the long-term viability of the product. The performance analysis is typically the focus of the standard review on PV cooling. However, there is rarely discussion of the crucial and accepted indicators to assess the effectiveness of cooling photovoltaic techniques such as the temperature-dependent PV efficiency difference factor (F_{TDED}), temperature-dependent photovoltaic power difference factor (F_{TDPD}), PV power difference factor (F_{ED}), power ratio (R), PV cooler lifespan efficacy factor (F_{LSE}), production cost effectiveness factor (F_{CE}), and modified production cost effectiveness factor (F_{MCE}), which are variables that can impact the PV cooling performance. Therefore, it is crucial to employ these methods to assess the effectiveness of PV enhancers. Table 4 describes each assessment method briefly.

Table 4. Comparison between performance assessment methods of PV enhancers.

Performance Factor	Equation	Description	Reference
Production cost effectiveness factor (F_{CE})	$F_{CE} = \frac{P_{PV} + \frac{Z}{Y}}{P_{PVCT}}$	This method links the manufacturing cost of the PV enhancer with the output power from adding an enhancer to the PV cell.	[83]
Modified production cost effectiveness factor (F_{MCE})	$F_{MCE} = \frac{n \times P_{cell} + \frac{Z}{Y}}{P_{PVCT}}$	This method can greatly reduce the assessment cost of PV enhancers.	[84]

Table 4. Cont.

Performance Factor	Equation	Description	Reference
PV cooling technique lifespan factor (F_{LSE})	$F_{LSE} = \frac{L_{PVCT}}{L_{PV}}$	The PV cooler lifespan effectiveness factor depends on the lifespan of both PV cell and cooler. This factor is defined as the ratio of the lifespan of the PV cooler to the lifespan of the PV cell. This technique is helpful in categorizing the performance of the PV cooler in terms of lifespan effectiveness.	[85]
PV efficiency difference factor (F_{TDED})	$F_{TDED} = \beta_{ref}(T_{PV} - T_{PVCT}) - \frac{P_{fc}}{P_{PV,max}}$	This parameter can indicate if the cooling technique is contributing to PV efficiency gain or loss, or is neutral, and may have the potential to be a measure of PV cooler performance evaluation by manufacturers and designers of PV coolers.	[86]
Modified PV efficiency difference factor (F_{TDPD})	$F_{TDPD} = \frac{\frac{1}{I_{STC}} [\beta_{ref}(T_{cell} - T_{PVCT})] - \frac{P_{fc}}{P_{PV,max}}}{R}$	This method has the flexibility to be applied under various solar irradiance values and depends on a PV module that has a single solar cell only, without a cooler.	[87]
PV power ratio (R)	$R = \frac{\frac{1}{I_{STC}} [1 - \beta_{ref}(T_{PVCT} - T_{ref})] - \frac{P_{fc}}{P_{PV,max}}}{R}$	This method instantly calculates the unknown power for different reference powers, and makes performance comparison among different enhancers simple.	[88]
PV power difference factor (F_{ED})	$F_{ED} = \frac{I_{STC}}{I} \left(\frac{P_{PVCT} - P_{fc} - n \times P_{cell}}{P_{PV,max}} \right)$	The method considers the power output of a standalone PV module with a single solar cell (without a cooler) as a reference point when evaluating the performance of a PV system containing a specified number of solar cells, equipped with a cooler. It can be used to evaluate the performance of different types of PV coolers.	[89]

3.4.1. Production Cost Effectiveness Factor (F_{CE})

In order to support the production of specific PV coolers based on their manufacturing cost and power productivity, an economic analysis was proposed. To achieve this, Sultan et al. proposed a parameter known as the PV cooling technique production cost effectiveness factor (F_{CE}). It defines and derives its value based on the power of a PV system both with and without a cooler, the cost of one watt of PV power, and the manufacturing cost of the PV cooler. This creates a relationship between the cost of manufacturing the cooler and its power productivity. To find the optimal type of PV cooler, the minimum value of F_{CE} is established. This method could be important in the classification and selection of PV cooling design during the manufacturing stages [83]. The F_{CE} can be represented as the following

$$F_{CE} = \frac{P_{PV} + \frac{Z}{Y}}{P_{PVCT}}, \quad (1)$$

where Z represents the cost of the cooling method and Y represents the cost of one watt of PV power. P_{PVCT} and P_{PV} are the output power from a PV module with and without a

cooler, respectively. The minimum value of F_{CE} , which indicates that the PV cooler has the optimum performance, is represented as the following

$$F_{CE,min} = \frac{P_{PV}}{P_{PVCT,max}}, \quad (2)$$

where $P_{PVCT,max}$ is the maximum output power from a PV module with an enhancer that is equivalent to the output power from a PV module at STC.

Based on Equation (1), F_{CE} has three possible conditions:

1. If $F_{CE} > 1$, it implies that the PV cooler is not production cost effective.
2. If $F_{CE} = 1$, it implies that the PV cooler is neutral and this is the threshold value.
3. If $F_{CE,min} \leq F_{CE} < 1$, it implies that the PV cooler is production cost effective.

Table 5 shows the effect of F_{CE} and its minimal value for various PV coolers. Assuming that a PV module with and without a cooler uses the same type of PV element, we may say that there are five different types of PV coolers: Type A, Type B, Type C, Type D, and Type E. Types A, B, and C yield 95, 102, and 105 W, respectively. However, Type D and Type E generate 120 and 140 W, respectively. The manufacturing costs of Type A, Type B, Type C, Type D, and Type E PV coolers are USD 20, 24, 25, 30, and 35, respectively, and the cost of one watt of PV power is USD 2. It is assumed that the value of $P_{PV,max}$ or $P_{PVCT,max}$ is 150 W. Through the implementation of F_{CE} and the utilization of Equation (1), PV coolers categorized as Type A, Type B, Type C, Type D, and Type E demonstrate F_{CE} values of 1.05, 1, 0.98, 0.88, and 0.77, respectively. Therefore, Type C, D, and E are production cost effective. Type A is not production cost effective and Type B is neutral. Using Equation (2), $F_{CE,min}$ is 0.6. Now Type E is the optimal design, because its F_{CE} value is the nearest to $F_{CE,min}$ value. It can be seen that F_{CE} can be used to evaluate the performance of PV coolers when manufacturing cost and power from PV modules with a cooler are considered [83].

Table 5. Example to compare different PV cooling techniques in terms of F_{CE} and $F_{CE,min}$. Reprinted with permission from Ref. [83]. Copyright 2019 John Wiley and Sons.

PV Cooler Type	$P_{PV,max}$, W	P_{PV} , W	P_{PVCT} , W	Cost of One Watt of PV Power, USD	Cost of PV Cooling Technique, USD	F_{CE}	$F_{CE,min}$	Production Cost Effectiveness
A	150	90	95	2	20	1.05	0.6	Not production cost effective
B	150	90	102	2	24	1	0.6	Neutral
C	150	90	105	2	25	0.98	0.6	Production cost effective
D	150	90	120	2	30	0.88	0.6	Production cost effective
E	150	90	140	2	35	0.77	0.6	Production cost effective

3.4.2. Modified Production Cost Effectiveness Factor (F_{MCE})

Again, Sultan et al. recently proposed a modified economic method to lower the cost of PV enhancer performance assessment. A single solar cell's output power without an enhancer, and the output power of a PV module with an enhancer that has a known number of solar cells, are the starting points for determining the modified production cost effectiveness factor (F_{MCE}) and its minimum value. Other factors include the cost of manufacturing the PV enhancer, the cost of one watt of PV power, and the output power for a PV module with and without an enhancer [84].

The modified production cost effectiveness factor (F_{MCE}) can be represented as follows:

$$F_{MCE} = \frac{n \times P_{cell} + Z}{P_{PVCT}} \quad (3)$$

It is evident that F_{MCE} is reliant on the subsequent entities:

1. The power output of a single solar cell (P_{cell}) in the absence of an enhancer.
2. The output power from a PV module with an enhancer, P_{PVCT} .
3. The quantity, n , of solar cells available in a PV module with an enhancer.
4. Z is the manufacturing cost of the PV enhancer.
5. The PV power's one-watt cost, Y .

The modified minimum value of F_{MCE} can be represented as the following

$$F_{MCE,min} = \frac{P_{cell}}{P_{cell,max}}, \quad (4)$$

where $P_{cell,max}$ is the output power from a solar cell at STC. The conditions of F_{MCE} are similar to F_{CE} conditions and are given in Section 3.4.1.

To examine the modified economic evaluation of PV enhancers, examples are given which are Type A and Type B PV enhancers. Tables 6 and 7 have been put together to show an economic evaluation of a PV module with Type A and Type B enhancers, utilizing the conventional and improved methodologies. However, one must first compute the cost of one watt of photovoltaic power. Let us assume that one watt of PV power costs MYR 13.40, and one PV set with the same number of solar cells as are available in a PV set with an enhancer is needed for the conventional method (F_{CE}). Two solar cells are present in our PV set with Type A and Type B. Therefore, two solar cells are required for the PV set without an enhancer in order to complete the economic analysis using F_{CE} . Given that the price of one solar cell is MYR 8.375, the cost of two solar cells comes to MYR 16.75 [84].

Table 6. The F_{CE} cost-effectiveness analysis for PV modules with Type A and Type B. Reprinted with permission from Ref. [84]. Copyright 2023 Elsevier.

PV Reflector	P_{cell}, W	P_{PVCT}, W	One Watt PV Power Cost, MYR	PV Enhancer Cost, MYR	F_{CE}	Remark	Assessment Cost (MYR)
Type A	0.374	0.579	13.40	2.30	0.942	Cost effective	35.8
Type B	0.374	0.592	13.40	4.60	1.212	Not cost effective	38.1

Table 7. The F_{MCE} cost-effectiveness analysis for PV modules with Type A and Type B. Reprinted with permission from Ref. [84]. Copyright 2023 Elsevier.

PV Enhancer	n	P_{cell}, W	P_{PVCT}, W	One Watt PV Power Cost, MYR	PV Enhancer Cost, MYR	F_{CE}	Remark	Assessment Cost (MYR)
Type A	2	0.187	0.579	13.40	2.30	0.942	Cost effective	27.41
Type B	2	0.185	0.592	13.40	4.60	1.212	Not cost effective	29.71

Table 6 shows that the cost of a PV module with Type A, when assessed economically using the conventional method (F_{CE}), comes to MYR 35.8. This amount is the total of the costs associated with both the PV module and Type A enhancer. A PV module with Type B costs MYR 38.1. However, with the modified method (F_{MCE}), a single solar cell is sufficient

to carry out the economic analysis. The total cost of one solar cell plus the cost of a PV module with Type A is MYR 27.41 for an economic assessment of a PV module with Type A (Table 7), but the cost of a PV module with Type B is MYR 29.71. Compared to F_{CE} , it is demonstrated that F_{MCE} can save 23.4% and 22% of the economic evaluation cost for a PV module with Type A and Type B, respectively. The modified method is more cost-effective than the conventional one, as evidenced by the preceding results. Tables 6 and 7 further demonstrate that the values of F_{MCE} and F_{CE} are the same. This demonstrates that the F_{MCE} is applicable [84].

3.4.3. Temperature-Dependent Efficiency Difference Factor (F_{TDED})

A strategy for evaluating PV cooling methods is presented, which is predicated on the definition and derivation of a novel parameter known as the temperature-dependent PV efficiency difference factor (F_{TDED}). This component determines the pertinent parameters that affect efficiency, and results in an evaluation of the PV cooling method as a whole. This parameter may be used as an indicator by product designers and manufacturers to assess the performance of PV coolers by showing whether the cooling method is neutral, increasing, or decreasing PV efficiency [86]. F_{TDED} can be represented as the following

$$F_{TDED} = \beta_{ref}(T_{PV} - T_{PVCT}) - \frac{P_{fc}}{P_{PV,max}}, \quad (5)$$

where T_{PVCT} and T_{PV} are the temperature of a PV module with and without a cooling technique. β_{ref} is the reference efficiency decrease per unit increase in temperature. P_{fc} is the pumping requirement (for forced circulation mode). $P_{PV,max}$ is the maximum output power from a PV module at STC.

From Equation (5), F_{TDED} has three possible conditions:

1. If $F_{TDED} > 0$, it implies the cooling technique contributes to PV efficiency gain.
2. If $F_{TDED} = 0$, it implies the cooling technique contributes neither gain nor loss to the PV efficiency, and it is the threshold value of the gain.
3. If $F_{TDED} < 0$, it implies the cooling technique contributes to PV efficiency loss.

Table 8 shows the applicability of F_{TDED} . Examples A through E show the forced fluid circulation mode. Example A shows that a PV module with and without a cooling mechanism has temperatures of 30 °C and 45 °C, respectively. Based on Equation (5), the F_{TDED} is +0.014, a positive value that suggests the cooling method increases PV efficiency. Now, if the PV module temperature after using a cooling strategy is 33.15 °C (Example B), the cooling technique can lower the PV module's temperature without increasing or decreasing the PV efficiency because the F_{TDED} value is zero [86].

In contrast, the temperature differential ($T_{PV} - T_{PVCT}$) for the natural fluid circulation mode (Examples F–H) serves as the benchmark for F_{TDED} and, consequently, for any efficiency gain or loss in P_{PV} . Example F demonstrates that the PV cell temperatures are 30 °C and 45 °C, respectively, with and without a PV cooling strategy. The positive value of F_{TDED} indicates that the cooling technique is enhancing PV efficiency. Since there is no temperature difference in Example G, PV efficiency is neutral and the F_{TDED} is zero. Last but not least, Example H's temperature differential of −1 and F_{TDED} of −0.0045 suggest that the PV cooling method is causing a reduction in P_{PV} efficiency [86]. Based on the presented results, it can be noticed that the F_{TDED} may provide an overall evaluation of PV cooling strategies in either forced or natural fluid circulation mode. This information could be useful to product designers and manufacturers [86].

Table 8. Examples to illustrate the F_{TDED} analysis and the PV module's efficiency gain or loss. Reprinted with permission from Ref. [86]. Copyright 2019 Springer Nature.

Examples	Type of Fluid Circulation	T_{PV} , °C	T_{PVCT} , °C	$P_{PV,max}$, W	P_{fc} , W	F_{TDED}	PV Efficiency (Gain or Loss)
A	Forced	45	30	75	4	+0.0014	Gain
B	Forced	45	33.15	75	4	0	Neutral
C	Forced	45	40	75	4	-0.031	Loss
D	Forced	45	45	75	4	-0.053	Loss
E	Forced	45	46	75	4	-0.058	Loss
F	Natural	45	30	75	0	+0.068	Gain
G	Natural	45	45	75	0	0	Neutral
H	Natural	45	46	75	0	-0.045	Loss

3.4.4. Temperature Dependent Photovoltaic Power Difference Factor (F_{TDPD})

The number of solar cells in a PV module has a direct correlation to its cost; as the number of solar cells increases, so does the cost of the PV module. Because the same total of solar cells is needed for a PV module with and without a cooler, the performance becomes expensive. To put it one way, if a PV module with a cooling method that uses 100 solar cells is utilized, then a PV module without a cooler should have the same number of solar cells, making a total of 200 solar cells necessary. Thus, a novel technique that may be used to minimize the cost of PV cooler performance assessment which relies on the output power of a PV module with just one solar cell without a cooler is suggested [86]. Also, this method has the flexibility to be applied under various levels of solar irradiance. The temperature dependent photovoltaic power difference factor, or F_{TDPD} , can be expressed as the following

$$F_{TDPD} = \frac{I}{I_{STC}} [\beta_{ref}(T_{cell} - T_{PVCT})] - \frac{P_{fc}}{P_{PV,max}}, \quad (6)$$

where I and I_{STC} are the solar irradiance and STC solar irradiance, that is 1000 W/m^2 , respectively. The conditions of F_{TDPD} are similar to F_{TDED} conditions and are given in Section 3.4.3.

Table 9 illustrates the impact of F_{TDPD} at 800 W/m^2 . It is noticed that F_{TDPD} values are 0.058, 0.032, 0.022, -0.0533 , -0.0713 , 0.054, 0, and -0.0036 for Types A, B, C, D, E, F, G, and H coolers, respectively. As a result, Types A, B, C, and F coolers contribute to photovoltaic efficiency gain. On the other hand, Types D, E, and H coolers contribute to photovoltaic efficiency loss, while the Type G cooler is neutral (at threshold value). It can be concluded that F_{TDPD} can be used to evaluate the performance of PV coolers.

Table 9. Cases to demonstrate F_{TDPD} analysis at I of 800 W/m^2 [87]. Reprinted with permission from Ref. [87]. Copyright 2022 Elsevier.

PV Cooler Types	Cooling Type	T_{cell} , °C (a Single Solar Cell without a Cooler)	T_{PVCT} , °C (a PV Cell with a Cooler)	F_{TDPD}	PV Efficiency Gain/Loss/Neutral
A	Forced	55	24	0.0583	Gain
B	Forced	55	31.3	0.0320	Gain
C	Forced	55	34	0.0223	Gain
D	Forced	55	55	-0.0533	Loss
E	Forced	55	60	-0.0713	Loss

Table 9. Cont.

PV Cooler Types	Cooling Type	T_{cell} , °C (a Single Solar Cell without a Cooler)	T_{PVCT} , °C (a PV Cell with a Cooler)	F_{TDPD}	PV Efficiency Gain/Loss/Neutral
F	Natural	55	40	0.054	Gain
G	Natural	55	55	0	Neutral
H	Natural	55	56	-0.0036	Loss

3.4.5. Power Difference Factor (F_{ED})

Another approach to reduce the PV cooler performance evaluation cost is the efficiency difference factor (F_{ED}). Under different levels of solar radiation, F_{ED} can carry out performance evaluation of PV coolers. When performing the performance evaluation for a PV module with a cooler that has a known number of solar cells, it also depends on the output power of a PV module with a single solar cell only. F_{ED} can be represented as the following:

$$F_{ED} = \frac{I_{STC}}{I} \left(\frac{P_{PVCT} - P_{fc} - n \times P_{cell}}{P_{PV,max}} \right) \quad (7)$$

The expression for the natural convection cooling becomes

$$F_{ED} = \frac{I_{STC}}{I} \left(\frac{P_{PVCT} - n \times P_{cell}}{P_{PV,max}} \right) \quad (8)$$

The F_{ED} is obviously dependent upon the following:

1. P_{cell} , which is the power output from a single solar cell in the absence of a cooler.
2. The PV output power from a PV module with a cooler, P_{PVCT} .
3. The PV output power at STC, $P_{PV,max}$.
4. The available solar cell count in a PV module with a cooler, n .
5. The pumping power, P_{fc} .
6. I , which is the solar irradiation.
7. I_{STC} , which is the solar irradiation at 1000 W/m².

The conditions of F_{ED} are similar to F_{TDED} conditions and are given in Section 3.4.3.

Numerical analysis was done by Sultan et al. to show the application of the F_{ED} factor (see Table 10). Examples A through D show the forced convection mode of cooling. In Example A, a single solar cell's output power (without cooling) is assumed to be 0.333 W, and the output power of a PV module with a cooler with 150 total solar cells is 60 W. Using Equation (7), the F_{ED} values are positive at +0.08 and +0.1 for incident solar irradiance levels of 1000 and 800 W/m², respectively. This suggests that the PV cooler is adding to the increase in photovoltaic efficiency. When a photovoltaic module with a cooler has 54 W of power, as demonstrated in Example B, F_{ED} values are zero for solar irradiance levels of 1000 and 800 W/m², meaning the PV cooler has no effect on photovoltaic efficiency. Now, in Example C, if a PV module with a cooler has a power of 52 W, the F_{ED} values at 1000 and 800 W/m² of solar irradiance values, respectively, are -0.026 and -0.033. These negative values suggest that the PV cooler is a contributing factor to the loss of photovoltaic efficiency [89].

In example D, a 45 W PV module with a cooler is used. At solar irradiance values of 1000 and 800 W/m², the F_{ED} values are -0.12 and -0.15, respectively. These negative values show that the PV cooler is not increasing photovoltaic efficiency. Conversely, for the natural convection mode (Examples E–G), Equation (8) is used. The reference point for the F_{ED} sign is the power difference ($P_{PVCT} - n \times P_{cell}$). When a PV system with a cooler in Example E has a power of 60 W, positive F_{ED} values (+0.13 and +0.163) at solar irradiance levels of 1000 and 800 W/m², respectively, are observed. This suggests that the cooler can enhance photovoltaic efficiency. Example F demonstrates that, for solar irradiance

levels of 1000 and 800 W/m², the F_{ED} values are zero since there is no power differential, which makes photovoltaic efficiency neutral. In conclusion, Example G demonstrates a 5 W power differential and F_{ED} values of -0.07 and -0.088 at 1000 and 800 W/m² solar irradiance, respectively. These results suggest that the cooler causes a loss rather than a gain in photovoltaic efficiency. It is demonstrated that F_{ED} works in different solar irradiance scenarios and can greatly reduce the evaluation cost, since one solar cell only (without cooling) is needed for the performance assessment for PV coolers [89].

Table 10. The F_{ED} analysis results at solar irradiance values of 800 and 1000 W/m².

PV Cooler Types	Cooling Type	P_{cell} , W	P_{PVCT} , W	$P_{PV,max}$, W	P_{fc} , W	F_{ED} at 1000 W/m ²	F_{ED} at 800 W/m ²	PV Efficiency Gain/Loss/Neutral
A	Forced	0.333	60	75	4	+0.08	+0.1	Gain
B	Forced	0.333	54	75	4	0	0	Neutral
C	Forced	0.333	52	75	4	-0.026	-0.033	Loss
D	Forced	0.333	45	75	4	-0.12	-0.15	Loss
E	Natural	0.333	60	75	0	+0.13	+0.163	Gain
F	Natural	0.333	50	75	0	0	0	Neutral
G	Natural	0.333	45	75	0	-0.07	-0.088	Loss

3.4.6. Power Ratio (R)

It is necessary to use the same PV reference power in order to compare cooler performance with natural convection, which makes the operation time-consuming. As a result, an evaluation technique is put forth, based on the defined and derived power ratio of the temperature-dependent photovoltaic module (R). The power of a PV module with a cooler and the reference power at STC for PV output are two examples of the pertinent metrics that are identified by R and are crucial for assessing the cooler's performance. Thus, rather than requiring the time-consuming procedure that the conventional method entails, the unknown power for various reference powers can be calculated instantaneously, and comparing the performance of various coolers is made simple. It is demonstrated that R produces identical outcomes to the current approach, which has undergone experimental validation [88].

As can be seen from Equation (9), R depends on the following: the temperature of a PV module after adding a cooler, T_{PVCT} ; the reference PV temperature, T_{ref} ; the reference fractional decrease in PV efficiency per unit increase in temperature, β_{ref} ; the pumping requirement, P_{fc} ; the maximum PV output power at STC, $P_{PV,max}$; the incident solar irradiation, I; and the solar irradiation at STC, I_{STC} . R can be denoted as the following:

$$R = \frac{I}{I_{STC}} [1 - \beta_{ref}(T_{PVCT} - T_{ref})] - \frac{P_{fc}}{P_{PV,max}}. \quad (9)$$

If P_{fc} has no influence or if convection cooling occurs naturally, the equation will become as shown in Ref. [88].

$$R = \frac{I}{I_{STC}} [1 - \beta_{ref}(T_{PVCT} - T_{ref})]. \quad (10)$$

In order to see the application of the power ratio, a study case was constructed by Sultan et al. It assumed that the temperatures of the PV coolers, or T_{PVCT} , are 30 °C for Type A, 27 °C for Type B, and 29 °C for Type C, as indicated in Table 11, in order to investigate the impact of the PV cooler's temperature on R. $P_{PV,max}$, T_{ref} , and β_{ref} have values of 340 W, 25 °C, and 0.0039 °C⁻¹, respectively. I and I_{STC} values are both 1000 W/m². For Type A, Type B, and Type C, the pumping power, P_{fc} , values are 0, 4, and 1 W, respectively. The new values of R, based on Equation (9), are 0.9805, 0.9804, and 0.9815

for Type A, Type B, and Type C PV coolers, respectively. It is noted that the Type C PV cooler has a higher R value as compared with Type A and Type B. As a result, it has the highest PV performance [88]. Now, when $P_{PV,max}$ value increases to 350 W, as shown in Table 12, the R values for PV coolers using natural cooling will be the same and changed for coolers with forced cooling.

Table 11. Cases to illustrate the analysis of R. Reprinted with permission from Ref. [88]. Copyright 2020 Elsevier.

PV Cooler Types	T_{PVCT} , °C	P_{fc} , W	T_{ref} , °C	β_{ref} , °C ⁻¹	$P_{PV,max}$, W	R
A	30	0	25	0.0039	340	0.9805
B	27	4	25	0.0039	340	0.9804
C	29	1	25	0.0039	340	0.9815

Table 12. Cases to illustrate the analysis of R when $P_{PV,max}$ is increased. Reprinted with permission from Ref. [88]. Copyright 2020 Elsevier.

PV Cooler Types	T_{PVCT} , °C	P_{fc} , W	T_{ref} , °C	β_{ref} , °C ⁻¹	$P_{PV,max}$, W	R
A	30	0	25	0.0039	300	0.9805
B	27	4	25	0.0039	300	0.9789
C	29	1	25	0.0039	300	0.9810

The performance of a PV cooler is demonstrated to be positively correlated with its R value, which remains constant for PV coolers operating in natural convection mode, irrespective of the PV reference power. When the PV reference power varies, the forced convection cooling R value also varies [88].

3.4.7. Lifespan Efficacy Factor (F_{LSE})

The lifespan of the PV cooler is a crucial factor that needs to be considered in order to justify the production of such products. By creating the PV cooler lifespan efficacy factor (F_{LSE}), whose value depends on the longevity of the PV module and the cooling method being used, the PV cooler's performance can be assessed. The ratio of the PV cooler's lifespan (L_{PVCT}) to the PV module's lifespan (L_{PV}) is F_{LSE} , which is useful in classifying the performance of PV coolers in terms of lifespan efficacy [85]. F_{LSE} can be represented as follows:

$$F_{LSE} = \frac{L_{PVCT}}{L_{PV}} \quad (11)$$

The following F_{LSE} criteria can be determined:

1. The PV cooler is considered to be lifespan effective if $0 < F_{LSE} \leq 1$.
2. The PV cooler is said to have maximum performance and longevity if $F_{LSE} = 1$.
3. The PV cooler performs the worst and has no lifespan effectiveness if $F_{LSE} = 0$.

Table 13 illustrates the F_{LSE} conditions. Let us assume that the lifespans of Type A, Type B, and Type C coolers are 7, 15, and 23 years, respectively. The same kind of PV module, which has a 15-year lifespan, is used in these PV coolers. The PV cooler lifespan efficacy factor values for Type A and Type B, derived from Equation (11), are 0.46, and 1, respectively. Because the PV cooler's lifespan is shorter than the PV module's, Type A's F_{LSE} value is less than unity. However, since the lifetime of the PV cooler and the PV module itself are equal, the F_{LSE} value for Type B is unity. According to the F_{LSE} definition, in order to obtain the F_{LSE} value for Type C, the lifespan of type C should be modified to match the PV module's lifespan, as it is crucial to have a PV cooler that can keep the PV module cool throughout its existence. Currently, Type C's F_{LSE} value is 1. Because all PV cooler types have F_{LSE} values between 0 and 1, it can be observed that they

are all lifespan effective ($0 < F_{LSE} \leq 1$). The highest F_{LSE} levels are found in Types B and C. From the perspective of lifespan effectiveness, they outperform Type A. It is observed that the performance assessment and comparison of various PV cooler types are facilitated by the application of F_{LSE} [85].

Table 13. Comparison of PV coolers using the PV cooler lifespan effectiveness factor [85].

PV Cooler Type	L_{PVCT} , Years	L_{PV} , Years	F_{LSE}	Performance Remark
Type A	7	15	0.467	Lifespan effective
Type B	15	15	1	Lifespan effective
Type C	23 *	15	1	Lifespan effective

* The lifespan of the PV cooler will be adjusted to have the same value as the PV module's lifespan.

4. Conclusions

In conclusion, PV cooling technologies play a crucial role in maximizing the efficiency and performance of photovoltaic (PV) solar panels. By effectively managing panel temperatures, these cooling methods help mitigate efficiency losses associated with heat buildup, ultimately optimizing energy production and enhancing the economic viability of solar energy systems. Whether through passive, active, or combined cooling approaches, the goal remains the same: to maintain PV panels within an optimal temperature range to ensure consistent and reliable electricity generation. The assessment methods for calculating the performance of PV cooling in different aspects, such as economic, power efficiency, lifespan of the PV module, and so on, are reviewed. These assessment methods are PV cooling technique lifespan factor (F_{LSE}), PV efficiency difference factor (F_{TDED}), modified PV efficiency difference factor (F_{TDPD}), PV power ratio (R), power difference factor (F_{ED}), production cost effectiveness factor (F_{CE}), and modified production cost effectiveness factor (F_{MCE}). A comparison and case studies are provided for each assessment method, which are rarely discussed in the previous literature. These assessment methods can be used by researchers and/or manufacturers of PV cooling techniques. It could be stated that as research and innovation continue to advance in this field, addressing challenges such as cost-effectiveness, maintenance requirements, and performance under extreme conditions will be essential to further improving the effectiveness and widespread adoption of PV cooling solutions. Overall, PV cooling represents a critical component in the ongoing transition towards sustainable and renewable energy sources.

Author Contributions: Conceptualization, I.O.H. and S.M.S.; methodology, I.O.H. and S.M.S.; software, I.O.H. and S.M.S.; validation, I.O.H. and S.M.S.; formal analysis, I.O.H. and S.M.S.; investigation, I.O.H. and S.M.S.; resources, I.O.H. and S.M.S.; data curation, I.O.H. and S.M.S.; writing—original draft preparation, I.O.H. and S.M.S.; writing—review and editing, I.O.H., S.M.S., C.P.T., A.F., M.M. and A.I.; visualization, I.O.H. and S.M.S.; supervision, S.M.S.; project administration, S.M.S.; funding acquisition, C.P.T. All authors have read and agreed to the published version of the manuscript.

Funding: This research was funded by Universiti Kebangsaan Malaysia, grant number GGPM-2023-028, and the APC was funded by Multimedia University.

Conflicts of Interest: The authors declare no conflicts of interest.

Abbreviations

Nomenclature

β	efficiency decrease per unit increase in temperature, ($^{\circ}\text{C}^{-1}$)
F	factor, dimensionless
I	solar irradiance, (W/m^2)
L	lifespan, (Year)
N	number of solar cells

STC	standard test condition
P	power, (W)
R	ratio, dimensionless
T	temperature, ($^{\circ}$ C)
Y	cost of one watt of PV (USD)
Z	cost of the cooling technique (USD)
Subscripts	
CE	photovoltaic module
Cell	cooling technique
ED	production cost effective
LSE	photovoltaic cell
max	PV power difference
min	lifespan effectiveness
PV	maximum output power
PVCT	minimum
ref	photovoltaic module with a cooler
TDED	reference
TDPD	PV efficiency difference factor
	PV power difference factor

References

- Nasr, E.A.; Mahmoud, H.A.; El-Meligy, M.A.; Awwad, E.M.; Salunkhe, S.; Naranje, V.; Swarnalatha, R.; Qudeiri, J.E.A. Electrical efficiency investigation on photovoltaic thermal collector with two different coolants. *Sustainability* **2023**, *15*, 6136. [[CrossRef](#)]
- Ibrahim, S.I.; Ali, A.H.; Hafidh, S.A.; Chaichan, M.T.; Kazem, H.A.; Ali, J.M.; Isahak, W.N.R.; Alamiery, A. Stability and thermal conductivity of different nanocomposite material prepared for thermal energy storage applications. *South Afr. J. Chem. Eng.* **2022**, *39*, 72–89. [[CrossRef](#)]
- Al-Maamary, H.M.; Kazem, H.A.; Chaichan, M.T. Climate change: The game changer in the Gulf Cooperation Council region. *Renew. Sustain. Energy Rev.* **2017**, *76*, 555–576. [[CrossRef](#)]
- Dano, U.L.; Abubakar, I.R.; Al-Shihri, F.S.; Ahmed, S.M.; Alrawaf, T.I.; Alshammari, M.S. A Multi-Criteria Assessment of Climate Change Impacts on Urban Sustainability in Dammam Metropolitan Area, Saudi Arabia. *Ain. Shams. Eng. J.* **2022**, *14*, 102062. [[CrossRef](#)]
- Kazem, H.A.; Al-Waeli, A.H.A.; Chaichan, M.T.; Sopian, K.; Ahmed, A.; Wan Nor Roslam, W.I. Enhancement of photovoltaic module performance using passive cooling (Fins): A comprehensive review. *Case Stud. Therm. Eng.* **2023**, *49*, 103316. [[CrossRef](#)]
- Azad, A.K.; Parvin, S. Photovoltaic thermal (PV/T) performance analysis for different flow regimes: A comparative numerical study. *Int. J. Thermof.* **2023**, *18*, 100319. [[CrossRef](#)]
- Al-Waeli, A.H.; Kazem, H.A.; Chaichan, M.T.; Sopian, K. *Photovoltaic/Thermal (PV/T) Systems: Principles, Design, and Applications*; Springer Nature: Berlin/Heidelberg, Germany, 2019.
- Pathak, P.K.; Roy, D.G.; Yadav, A.K.; Padmanaban, S.; Blaabjerg, F.; Khan, B. A State-of-the-Art Review on Heat Extraction Methodologies of Photovoltaic/Thermal System. *IEEE Access* **2023**, *11*, 49738–49759. [[CrossRef](#)]
- Jehad, A.; Alaa, F.; Ahmed, A. Temperature effect on performance of different solar cell technologies. *J. Ecol. Eng.* **2019**, *20*, 249–254.
- Kazem, H.A. Evaluation of aging and performance of grid-connected photovoltaic system northern Oman: Seven years' experimental study. *Sol. Energy* **2021**, *207*, 1247–1258. [[CrossRef](#)]
- Suresh, A.K.; Khurana, S.; Nandan Gopal Dwivedi, G.; Kumar, G. Role on nanofluid in cooling solar photovoltaic cell to enhance overall efficiency. *Mater. Today Proc.* **2018**, *5*, 20614–20620. [[CrossRef](#)]
- Bhakre, S.S.; Sawarkar, P.D.; Kalamkar, V.R. Performance evaluation of PV panel surfaces exposed to hydraulic cooling—A review. *Sol. Energy* **2021**, *224*, 1193–1209. [[CrossRef](#)]
- Sajan, P. Water and phase change material based photovoltaic thermal management systems: A review. *Renew. Sustain. Energy Rev.* **2018**, *82*, 791–807. [[CrossRef](#)]
- Elbreki, A.M.; Alghoul, M.A.; Sopian, K.; Hussein, T. Towards adopting passive heat dissipation approaches for temperature regulation of PV module as a sustainable solution. *Renew. Sustain. Energy Rev.* **2017**, *69*, 961–1017. [[CrossRef](#)]
- Bahaidarah, H.M.S.; Baloch, A.A.B.; Gandhidasan, P. Uniform cooling of photo-voltaic panels: A review. *Renew. Sustain. Energy Rev.* **2016**, *57*, 1520–1544. [[CrossRef](#)]
- Ghadikolaei, S.S.C. Solar photovoltaic cells performance improvement by cooling Technology: An overall review. *Int. J. Hydrg. Energy* **2021**, *46*, 10939–10972. [[CrossRef](#)]
- Verma, S.; Mohapatra, S.; Chowdhury, S.; Dwivedi, G. Cooling techniques of the PV module: A review. *Mater. Today Proc.* **2020**, *38*, 253–258. [[CrossRef](#)]

18. Glunz, S.; Preu, R. Crystalline silicon solar cells—State-of-the-art and future developments. In *Comprehensive Renewable Energy*, 2nd ed.; Elsevier: Amsterdam, The Netherlands, 2022; pp. 293–324. [[CrossRef](#)]
19. Rahman, M.M.; Hasanuzzaman, M.; Rahim, N.A. Effects of various parameters on PV-module power and efficiency. *Energy Convers. Manag.* **2015**, *103*, 348–358. [[CrossRef](#)]
20. Elnozahy, A.; Abd-Elbary, H.; Abo-Elyousr, F.K. Efficient energy harvesting from PV Panel with reinforced hydrophilic nano-materials for eco-buildings. *Energy Built Environ.* **2024**, *5*, 393–403. [[CrossRef](#)]
21. Hu, M.; Zhao, B.; Ao, X.; Cao, J.; Wang, Q.; Riffat, S.; Su, Y.; Pei, G. Effect of the spectrally selective features of the cover and emitter combination on radiative cooling performance. *Energy Built Environ.* **2021**, *2*, 251–259. [[CrossRef](#)]
22. Mamun, M.; Islam, M.; Hasanuzzaman, M.; Selvaraj, J. Effect of tilt angle on the performance and electrical parameters of a PV module: Comparative indoor and outdoor experimental investigation. *Energy Built Environ.* **2022**, *3*, 278–290. [[CrossRef](#)]
23. Mangkuto, R.A.; Tresna, D.N.A.T.; Hermawan, I.M.; Pradipta, J.; Jamala, N.; Paramita, B.; Athaillah. Experiment and simulation to determine the optimum orientation of building-integrated photovoltaic on tropical building façades considering annual daylight performance and energy yield. *Energy Built Environ.* **2024**, *5*, 414–425. [[CrossRef](#)]
24. Yadav, K.; Kumar, B.; Swaroop, D. Mitigation of mismatch power losses of PV array under partial shading condition using novel odd even configuration. *Energy Rep.* **2020**, *6*, 427–437. [[CrossRef](#)]
25. Thoy, E.; Wen, J.; Go, Y.L. Enhancement and validation of building integrated PV system: 3D modelling, techno-economics and environmental assessment. *Energy Built Environ.* **2021**, *3*, 444–466. [[CrossRef](#)]
26. Gharzi, M.; Arabhosseini, A.; Gholami, Z.; Rahmati, M.H. Progressive cooling technologies of photovoltaic and concentrated photovoltaic modules: A review of fundamentals, thermal aspects, nanotechnology utilization and enhancing performance. *Sol. Energy* **2020**, *211*, 117–146. [[CrossRef](#)]
27. Ahmad, E.; Fazlizan, A.; Jarimi, H.; Sopian, K.; Ibrahim, A. Enhanced heat dissipation of truncated multi-level fin heat sink (MLFHS) in case of natural convection for photovoltaic cooling. *Case Stud. Therm. Eng.* **2021**, *28*, 101578. [[CrossRef](#)]
28. Akrouch, M.A.; Chahine, K.; Faraj, J.; Hachem, F.; Castelain, C.; Khaled, M. Advancements in cooling techniques for enhanced efficiency of solar photovoltaic panels: A detailed comprehensive review and innovative classification. *Energy Built Environ.* **2023**; In press. [[CrossRef](#)]
29. Demir, M.; Omeroglu, G.; Ozakin, A.N. Experimental determination of the effect of fins of different cylindrical geometries on electrical and thermal efficiency in an air-cooled PVT system. *Heat Tran. Res.* **2023**, *54*, 1–16. [[CrossRef](#)]
30. Marinić-Kragić, I.; Nižetić, S.; Grubišić-Čabo, F.; Čoko, D. Analysis and optimization of passive cooling approach for free-standing PV panel: Introduction of slits. *Energy Convers. Manag.* **2020**, *204*, 112277. [[CrossRef](#)]
31. Bayrak, F.; Oztop, H.F.; Selimefendigil, F. Effects of different fin parameters on temperature and efficiency for cooling of photovoltaic panels under natural convection. *Sol. Energy* **2019**, *188*, 484–494. [[CrossRef](#)]
32. Ma, T.; Li, Z.; Zhao, J. Photovoltaic panel integrated with phase change materials (PV-PCM): Technology overview and materials selection. *Renew. Sustain. Energy Rev.* **2019**, *116*, 109406. [[CrossRef](#)]
33. Nazir, H.; Batool, M.; Bolivar, O.F.J.; Isaza-Ruiz, M.; Xu, X.; Vignarooban, K. Recent developments in phase change materials for energy storage applications: A review. *Int. J. Heat Mass Transf.* **2019**, *129*, 491–523. [[CrossRef](#)]
34. Pandey, A.; Hossain, M.; Tyagi, V.; Rahim, N.A.; Jeyraj, A.; Selvaraj, L. Novel approaches and recent developments on potential applications of phase change materials in solar energy. *Renew. Sustain. Energy Rev.* **2018**, *82*, 281–323. [[CrossRef](#)]
35. Sandro, N.; Miso, J.; Duje, C.; Müslüm, A. A novel and effective passive cooling strategy for PV panel. *Renew. Sustain. Energy Rev.* **2021**, *145*, 111164.
36. Tian, D.; Shi, T.; Wang, X.; Liu, H.; Wang, X. Magnetic field-assisted acceleration of energy storage based on microencapsulation of phase change material with $\text{CaCO}_3/\text{Fe}_3\text{O}_4$ composite shell. *J. Energy Storage* **2022**, *47*, 103574. [[CrossRef](#)]
37. Rezvanpour, M.; Borooghani, D.; Farschad, T.; Maryam, P. Using $\text{CaCl}_2 \cdot 6\text{H}_2\text{O}$ as a phase change material for thermo-regulation and enhancing PV panels' conversion efficiency experimental study and TRNSYS validation. *Renew. Energy* **2020**, *146*, 1907–1921. [[CrossRef](#)]
38. Abo-Elour, F.; Zeidan, E.B.; Sultan, A.A.; El-Negiry, E.; Soliman, A.S. Enhancing the bifacial PV system by using dimples and multiple PCMs. *J. Energy Storage* **2023**, *70*, 108079. [[CrossRef](#)]
39. Ranawade, V.; Nalwa, K.S. Multilayered PCMs-based cooling solution for photovoltaic modules: Modelling and experimental study. *Renew. Energy* **2023**, *216*, 119136. [[CrossRef](#)]
40. Maghrabie, H.M.; Mohamed, A.S.A.; Fahmy, A.M.; Samee, A.A.A. Performance enhancement of PV panels using phase change material (PCM): An experimental implementation. *Case Stud. Therm. Eng.* **2023**, *42*, 102741. [[CrossRef](#)]
41. Yao, H.; Pu, W.; Wang, J.; Qin, Y.; Qiao, L.; Song, N. A novel thermosyphon cooling applied to concentrated photovoltaic-thermoelectric system for passive and efficient heat dissipation. *Appl. Therm. Eng.* **2024**, *236 Pt A*, 121460. [[CrossRef](#)]
42. Moradgholi, M.; Nowee, S.M.; Farzaneh, A. Experimental study of using Al_2O_3 /methanol nanofluid in a two-phase closed thermosyphon (TPCT) array as a novel photovoltaic/thermal system. *Sol. Energy* **2018**, *164*, 243–250. [[CrossRef](#)]
43. Wang, H.; Qu, J.; Sun, Q.; Kang, Z.; Han, X. Thermal characteristic comparison of three-dimensional oscillating heat pipes with/without sintered copper particles inside flat-plate evaporator for concentrating photovoltaic cooling. *Appl. Therm. Eng.* **2020**, *167*, 114815. [[CrossRef](#)]
44. He, J.; Li, K.; Jia, L.; Zhu, Y.; Zhang, H.; Linghu, J. Advances in the applications of thermoelectric generators. *Appl. Therm. Eng.* **2024**, *236 Pt D*, 121813. [[CrossRef](#)]

45. Jaziri, N.; Boughamoura, A.; Müller, J.; Mezghani, B.; Tounsi, F.; Ismail, M. A comprehensive review of Thermoelectric Generators: Technologies and common applications. *Energy Rep.* **2020**, *6*, 264–287. [[CrossRef](#)]
46. Champier, D. Thermoelectric generators: A review of applications. *Energy Convers. Manag.* **2017**, *140*, 167–181. [[CrossRef](#)]
47. Yin, E.S.; Li, Q.; Xuan, Y.M. Feasibility analysis of a tandem photovoltaic-thermoelectric hybrid system under solar concentration. *Renew. Energy* **2020**, *162*, 1828–1841. [[CrossRef](#)]
48. Yaya, L.; Han, X.; Chen, X.; Yao, Y. Maximizing energy output of a vapor chamber-based high concentrated PV-thermoelectric generator hybrid system. *Energy* **2023**, *282*, 128882. [[CrossRef](#)]
49. Elbreki, A.M.; Muftah, A.F.; Sopian, K.; Jarimi, H.; Fazlizan, A.; Ibrahim, A. Experimental and economic analysis of passive cooling PV module using fins and planar reflector. *Case Stud. Therm. Eng.* **2021**, *23*, 100801. [[CrossRef](#)]
50. Hernandez-Perez, J.G.; Carrillo, J.G.; Bassam, A.; Flota-Banuelos, M.; Patino-Lopez, L.D. A new passive PV heatsink design to reduce efficiency losses: A computational and experimental evaluation. *Renew. Energy* **2020**, *147*, 1209–1220. [[CrossRef](#)]
51. Nada, S.A.; El-Nagar, D.H.; Hussein, H.M.S. Improving the thermal regulation and efficiency enhancement of PCM-Integrated PV modules using nano particles. *Energy Convers. Manag.* **2018**, *166*, 735–743. [[CrossRef](#)]
52. Elsheniti Mahmoud, B.; Hemedah Moataz, A.; Sorour, M.M.; El-Maghly Wael, M. Novel enhanced conduction model for predicting performance of a PV panel cooled by PCM. *Energy Convers. Manag.* **2020**, *205*, 112456. [[CrossRef](#)]
53. Yesildal, F.; Ozakin, A.N.; Yakut, K. Optimization of operational parameters for a photovoltaic panel cooled by spray cooling. *Eng. Sci. Technol. Int. J.* **2022**, *25*, 100983. [[CrossRef](#)]
54. Kemal, B.; Ismail, E. Effects of cooling on performance of photovoltaic/thermal (PV/T) solar panels: A comprehensive. *Solar Energy* **2023**, *262*, 111829.
55. Shamroukh, A.N. Thermal regulation of photovoltaic panel installed in Upper Egyptian conditions in Qena. *Therm. Sci. Eng. Prog.* **2019**, *14*, 100438. [[CrossRef](#)]
56. Irwan, Y.M.; Leow, W.Z.; Irwanto, M.; Fareq, M.; Amelia, A.R.; Gomesh, N.; Safwati, I. Indoor test performance of PV panel through water cooling method. *Energy Procedia* **2015**, *79*, 604–611. [[CrossRef](#)]
57. Rahimi, M.; Asadi, M.; Karami, N.; Karimi, E. A comparative study on using single and multi-header microchannels in a hybrid PV cell cooling. *Energy Convers. Manag.* **2015**, *101*, 1–8. [[CrossRef](#)]
58. Peng, Z.; Herfatmanesh, M.R.; Liu, Y. Cooled solar PV panels for output energy efficiency optimization. *Energy Convers. Manag.* **2017**, *150*, 949–955. [[CrossRef](#)]
59. Ebaid, M.S.Y.; Ghrair, A.M.; Al-Busoul, M. Experimental investigation of cooling photovoltaic (PV) panels using (TiO_2) nanofluid in water–polyethylene glycol mixture and (Al_2O_3) nanofluid in water–cetyltrimethylammonium bromide mixture. *Energy Convers. Manag.* **2018**, *155*, 324–343. [[CrossRef](#)]
60. Nardi, I.; Ambrosini, I.; Rubeis, T.; Paoletti, D.; Muttillo, M.; Sfarra, S. Energetic performance analysis of a commercial water-based photovoltaic thermal system (PV/T) under summer conditions. *J. Phys. Conf. Ser.* **2017**, *923*, 012040. [[CrossRef](#)]
61. Bahaidarah, H.M.S. Experimental performance evaluation and modeling of jet impingement cooling for thermal management of photovoltaics. *Sol. Energy* **2016**, *135*, 605–617. [[CrossRef](#)]
62. Maatoug, S.; Moulahi, A.; Bazuhair, N.; Alqarni, S.; Selimefendigil, F.; Aich, W.; Kolsi, L.; Mhimid, A. Pulsating multiple nano-jet impingement cooling system design by using different nanofluids for photovoltaic (PV) thermal management. *Case Stud. Therm. Eng.* **2023**, *41*, 102650. [[CrossRef](#)]
63. Kianifard, S.; Zamen, M.; Nejad, A.A. Modeling, designing and fabrication of a novel PV/T cooling system using half pipe. *J. Clean. Prod.* **2020**, *253*, 119972. [[CrossRef](#)]
64. Liu, Y.; Chen, Y.; Wang, D.; Liu, J.; Luo, X.; Wang, Y.; Liu, H.; Liu, J. Experimental and numerical analyses of parameter optimization of photovoltaic cooling system. *Energy* **2020**, *215*, 119159. [[CrossRef](#)]
65. Pang, W.; Cui, Y.; Zhang, Q.; Yan, H. Building integrated photovoltaic module-based on aluminum substrate with forced water cooling. *J. Sol. Energy Eng.* **2018**, *140*, 021005. [[CrossRef](#)] [[PubMed](#)]
66. Alihosseini, Y.; Oghabneshin, Y.; Bari, A.R.; Moslemi, S.; Roozbehi, A.R.; Targhi, M.Z.; Guo, W. Performance of high-concentration photovoltaic cells cooled by a hybrid microchannel heat sink. *Appl. Therm. Eng.* **2024**, *238*, 122206. [[CrossRef](#)]
67. Elavarasan, R.M.; Mudgal, V.; Selvamanohar, L.; Wang, K.; Huang, G.; Shafiullah, G.M.; Markides, C.N.; Reddy, K.S.; Nadarajah, M. Pathways toward high-efficiency solar photovoltaic thermal management for electrical, thermal and combined generation applications: A critical review. *Energy Convers. Manag.* **2022**, *55*, 115278. [[CrossRef](#)]
68. Arifin, Z.; Tjahjana, D.D.D.P.; Hadi, S.; Rachmanto, R.A.; Setyohandoko, G.; Sutanto, B. Numerical and experimental investigation of air cooling for photovoltaic panels using aluminum heat sinks. *Int. J. Photoenergy* **2020**, *2020*, 1574274. [[CrossRef](#)]
69. Rahman, N.M.A.; Haw, L.C.; Kamaluddin, K.A.; Abdulla, M.S.I. Investigating photovoltaic module performance using aluminium heat sink and forced cold-air circulation method in tropical climate conditions. *Energy Rep.* **2023**, *9*, 2797–2809. [[CrossRef](#)]
70. Hussien, A.; Eltayesh, A.; El-Batsh, H.M. Experimental and numerical investigation for PV cooling by forced convection. *Alex. Eng. J.* **2023**, *64*, 427–440. [[CrossRef](#)]
71. Syafiqah, Z.; Irwan, Y.; Amin, N.; Irwanto, M.; Leow, W.; Amelia, A. Thermal and electrical study for PV panel with cooling. *Indones. J. Electr. Eng. Comput. Sci.* **2019**, *7*, 492–499. [[CrossRef](#)]
72. Dehghan, M.; Rahgozar, S.; Pourrajabian, A.; Aminy, M.; Halek, F.S. Techno-economic perspectives of the temperature management of photovoltaic (PV) power plants: A case-study in Iran. *Sustain. Energy Technol. Assess.* **2021**, *45*, 101133. [[CrossRef](#)]

73. Almuwailhi, A.; Zeitoun, O. Investigating the cooling of solar photovoltaic modules under the conditions of Riyadh. *J. King Saud Univers. Eng. Sci.* **2023**, *35*, 123–136. [[CrossRef](#)]
74. Rostami, Z.; Rahimi, M.; Azimi, N. Using high-frequency ultrasound waves and nanofluid for increasing the efficiency and cooling performance of a PV module. *Energy Convers. Manag.* **2018**, *160*, 141–149. [[CrossRef](#)]
75. Hadipour, A.; Zargarabadi, M.R.; Rashidi, S. An efficient pulsed-spray water cooling system for photovoltaic panels: Experimental study and cost analysis. *Renew. Energy* **2021**, *164*, 867–875. [[CrossRef](#)]
76. Babu, C.; Ponnambalam, P. The theoretical performance evaluation of hybrid PV-TEG system. *Energy Convers. Manag.* **2018**, *173*, 450–460. [[CrossRef](#)]
77. Hassan, A.; Wahab, A.; Qasim, M.A.; Janjua, M.M.; Ali, M.A.; Ali, H.M. Thermal management and uniform temperature regulation of PV modules using hybrid phase change materials-nanofluids system. *Renew. Energy* **2020**, *145*, 282–293. [[CrossRef](#)]
78. Yang, L.-H.; Liang, J.-D.; Hsu, C.-Y.; Yang, T.-H.; Chen, S.-L. Enhanced efficiency of PV panels by integrating a spray cooling system with shallow geothermal energy heat exchanger. *Renew. Energy* **2019**, *134*, 970–981. [[CrossRef](#)]
79. Elminshawy, N.A.S.; El Ghandour, M.; Gad, H.M.; El-Damhogi, D.G.; El-Nahhas, K.; Addas, M.F. The performance of a buried heat exchanger system for PV panel cooling under elevated air temperatures. *Geothermics* **2019**, *82*, 7–15. [[CrossRef](#)]
80. Idoko, L.; Anaya-Lara, O.; McDonald, A. Enhancing PV modules efficiency and power output using multi-concept cooling technique. *Energy Rep.* **2018**, *4*, 357–369. [[CrossRef](#)]
81. Sudhakar, P.; Santosh, R.; Asthalakshmi, B.; Kumaresan, G.; Velraj, R. Performance augmentation of solar photovoltaic panel through PCM integrated natural water circulation cooling technique. *Renew. Energy* **2021**, *172*, 1433–1448. [[CrossRef](#)]
82. Agyekum, E.B.; Seepana, P.K.; Naseer, T.A.; Vladimir, I.V.; Sergey, E.S. Effect of dual surface cooling of solar photovoltaic panel on the efficiency of the module: Experimental investigation. *Heliyon* **2021**, *7*, e07920. [[CrossRef](#)]
83. Sultan, S.M.; Tso, C.P.; Ervina, E.M.N. A new production cost effectiveness factor for assessing photovoltaic module cooling techniques. *Int. J. Energy Res.* **2020**, *44*, 574–583. [[CrossRef](#)]
84. Sultan, S.M.; Tso, C.P.; Ajeel, R.K.; Sobayel, K.; Abdullah, M.Z. A Detailed Analysis of the Modified Economic Method for Assessing the Performance of Photovoltaic Module Enhancing Techniques. *Sustainability* **2023**, *15*, 12028. [[CrossRef](#)]
85. Sultan, S.M.; Abdullah, M.Z. A new method for assessing photovoltaic module cooler based on lifespan effectiveness factor. *Case Stud. Therm. Eng.* **2022**, *35*, 102126. [[CrossRef](#)]
86. Sultan, S.M.; Tso, C.P.; Ervina, E.M.N. A Proposed temperature-dependent photovoltaic efficiency difference factor for evaluating photovoltaic module cooling techniques in natural or forced fluid circulation mode. *Arab. J. Sci. Eng.* **2019**, *44*, 8123–8128. [[CrossRef](#)]
87. Sultan, S.M.; Tso, C.P.; Ervina, E.M.N.; Abdullah, M.Z. Cost and time effective performance evaluation methods for photovoltaic module cooling techniques: Analytical and experimental study. *Sol. Energy* **2022**, *326*, 119940. [[CrossRef](#)]
88. Sultan, S.M.; Tso, C.P.; Ervina, E.M.N. A new approach for photovoltaic module cooling technique evaluation and comparison using the temperature dependent photovoltaic efficiency ratio. *Sustain. Energy Technol. Assess.* **2020**, *30*, 100705.
89. Sultan, S.M.; Tso, C.P.; Ervina, E.M.N. Anew method for reducing the performance evaluation cost of the photovoltaic module cooling techniques using the photovoltaic efficiency difference factor. *Case Stud. Therm. Eng.* **2020**, *21*, 100682. [[CrossRef](#)]

Disclaimer/Publisher’s Note: The statements, opinions and data contained in all publications are solely those of the individual author(s) and contributor(s) and not of MDPI and/or the editor(s). MDPI and/or the editor(s) disclaim responsibility for any injury to people or property resulting from any ideas, methods, instructions or products referred to in the content.